AD_____

AWARD NUMBER: W81XWH-05-1-0515

TITLE: Protease Mediated Anti-Cancer Therapy

PRINCIPAL INVESTIGATOR: Ching-Hsuan Tung

CONTRACTING ORGANIZATION: Massachusetts General Hospital
Boston, Massachusetts 02114-2554

REPORT DATE: August 2006

TYPE OF REPORT: Final

PREPARED FOR: U.S. Army Medical Research and Materiel Command
Fort Detrick, Maryland 21702-5012

REPORT DOCUMENTATION PAGE

Form Approved
OMB No. 0704-0188

1. REPORT DATE *(DD-MM-YYYY)*	**2. REPORT TYPE**	**3. DATES COVERED** *(From - To)*
01-08-2006	Final	1 Aug 2005 – 31 Jul 2006

4. TITLE AND SUBTITLE

Protease Mediated Anti-Cancer Therapy

5a. CONTRACT NUMBER

5b. GRANT NUMBER
W81XWH-05-1-0515

5c. PROGRAM ELEMENT NUMBER

6. AUTHOR(S)

Ching-Hsuan Tung

E-Mail: tung@helix.mgh.harvard.edu

5d. PROJECT NUMBER

5e. TASK NUMBER

5f. WORK UNIT NUMBER

7. PERFORMING ORGANIZATION NAME(S) AND ADDRESS(ES)

Massachusetts General Hospital
Boston, Massachusetts 02114-2554

8. PERFORMING ORGANIZATION REPORT NUMBER

9. SPONSORING / MONITORING AGENCY NAME(S) AND ADDRESS(ES)
U.S. Army Medical Research and Materiel Command
Fort Detrick, Maryland 21702-5012

10. SPONSOR/MONITOR'S ACRONYM(S)

11. SPONSOR/MONITOR'S REPORT NUMBER(S)

12. DISTRIBUTION / AVAILABILITY STATEMENT
Approved for Public Release; Distribution Unlimited

13. SUPPLEMENTARY NOTES

14. ABSTRACT

A new approach to selective photodynamic therapy (PDT) was developed by designing chlorin e6 containing macromolecules which are sensitive to tumor-associated proteases. The agents are non-toxic in their native state but become fluorescent and produce singlet oxygen (SOG) upon protease conversion. Coupled with optimized delivery systems we demonstrate that a) the agents efficiently accumulate in tumors due to the enhanced permeability and retention effect, b) the agents are locally activated by proteases, c) local drug concentrations can be measured by quantitative fluorescence tomography, and d) light treated tumors show reduced growth. A single low dose of PDT (0.125 mg Ce6 equivalent/kg) was sufficient to suppress tumor growth by over 50%. Activatable SOG agents provide increased efficacy with reduced toxicity, and it could become a powerful photodynamic therapy.

15. SUBJECT TERMS
No subject terms provided.

16. SECURITY CLASSIFICATION OF:			**17. LIMITATION OF ABSTRACT**	**18. NUMBER OF PAGES**	**19a. NAME OF RESPONSIBLE PERSON**
a. REPORT	**b. ABSTRACT**	**c. THIS PAGE**			USAMRMC
U	U	U	UU	24	**19b. TELEPHONE NUMBER** *(include area code)*

Table of Contents

Abstract:
A new approach to selective photodynamic therapy (PDT) was developed by designing chlorin e6 containing macromolecules which are sensitive to tumor-associated proteases. The agents are non-toxic in their native state but become fluorescent and produce singlet oxygen (SOG) upon protease conversion. Coupled with optimized delivery systems we demonstrate that a) the agents efficiently accumulate in tumors due to the enhanced permeability and retention effect, b) the agents are locally activated by proteases, c) local drug concentrations can be measured by quantitative fluorescence tomography, and d) light treated tumors show reduced growth. A single low dose of PDT (0.125 mg Ce6 equivalent/kg) was sufficient to suppress tumor growth by over 50%. Activatable SOG agents provide increased efficacy with reduced toxicity, and it could become a powerful photodynamic therapy.

Introduction
The goal of this proposal is to develop a highly potent cathepsin B (CaB) sensitive anti-cancer agent to treat breast cancer while minimizing unnecessary toxicity. Cytotoxic agents are shielded by a protease sensitive chemical linkage and these agents are non-toxic until they are activated by the selected proteases in the cancer-afflicted area. Using this approach, the nonspecific, whole body toxicity will be reduced and the regional concentration of the therapeutic agents can be significantly improved. We proposed to synthesize, characterize, in vitro evaluation and in vivo evaluation of the protease activatable therapeutic agents, and we have achieved all the proposed aims.

Body
1. Preparation and in vitro evaluation of protease mediated anti-cancer therapy
To demonstrate the concept, we coupled multiple chlorin e6 (Ce6) molecules onto a biodegradable poly-L-lysine grafted with monomethoxy-poly(ethylene glycol) (abbreviated as L-PGC) to induce aggregation and self-quenching while still representing a biocompatible agent with favorable tumor accumulating properties. After this initial optimization experiments, the preparation with 15 Ce6 molecules per L-PGC molecule (L-SR15) was the lead compound. L-PGC is a known substrate for cysteine protease, therefore L-SR15 was tested against several cysteine proteases, including cathepsins B, L and S, at pH 5.0. Among these 3 proteases, CaB induced the highest fluorescence. L-SR15 treated with CaB or L showed 4.0 (P=0.0007) or 1.6 (P=0.0012) times higher fluorescence intensities compared to control (buffer-treated L-SR15). The CaB inhibitor CA-074 completely inhibited fluorescence recovery upon CaB addition. Furthermore, a D-polylysine based PGC with similar substitution ratio (D-SR16) was also prepared and tested under identical conditions. Similar fluorescence quenching effect (~86 % quenching) was observed with the D-backbone; however, no noticeable fluorescence activation occurred upon CaB addition. The above results thus confirm that proteolytic degradation is indeed the primary mechanism of fluorescence activation.

Singlet oxygen generation of L-SR15 and D-SR16 was subsequently assayed using similar CaB incubation experiments. In the native state, SOG of L-SR15 was only 13%

compared to that of free Ce6 at equimolar concentrations. In the absence of CaB, the buffer containing L-SR15 remained quenched. Upon CaB treatment, SOG increased up to 79%, a 6-fold increase (P=0.0012). As with the fluorescence experiment, inhibitory effects were observed with CA-074 treatment. As expected, addition of CaB to D-SR16 showed no enhancement in SOG. These results, again, support the hypothesis that not only fluorescence but also SOG can be quenched and selectively recovered upon specific protease treatments.

2. Imaging in vivo activation.
The protease-mediated strategy was next examined *in vivo* using a xenographic tumor model. HT1080 cell line was selected for the animal study because of its high expressing level of CaB. HT-1080 human fibrosarcomas were subcutaneously implanted in mice. After intravenous injection of L-SR15 (0.125 mg Ce6 eq./kg), the fluorescence activation in tumors (n=6) were clearly imaged using fluorescence molecular tomography. There was accumulation of L-SR15 in tumor with time, reaching the highest concentration of 17.0 ± 1 nM at 24 hr post-injection. Using this imaging technology, the local concentration of the PS can be measured conveniently in real time. This pharmacokinetic information would be valuable to evaluate the delivery efficiency of pro-PS, and to plan the schedule of light irradiation.

In a separate set of animals, free Ce6, L-SR15 or D-SR16 (0.125 mg Ce6 eq./kg) were injected intravenously, tumors were collected and sectioned. These animals received no light treatment to preserve fluorescence signal. High fluorescence signal was observed in the animals injected with L-SR15, while D-SR16 and Ce6 injected groups showed little or no fluorescence signal. These results support that L-SR15 is activated in tumors *in vivo* similar as in the previous *in vitro* assays. Merged images showed that the fluorescence of L-SR15 fragments was distributed in cellular cytoplasm, but did not localize to the nucleus. On the contrary, D-SR16 treated animals did not show any significant fluorescence in tumors. Another interesting finding was that fluorescence signal of free Ce6 was much lower than that of L-SR15 injected animals. Polymeric drug carriers with polyethylene glycol grafting such as PGC conjugate have been shown prolonged blood circulation and higher accumulation in tumors by the enhanced permeability and retention (EPR) effect.

3. In vivo anti-tumor effect.
To demonstrate therapeutic efficacy *in vivo*, L-SR15 or D-SR16 (0.125 mg Ce6 eq./kg) in PBS was injected IV and 24 h later, animals were treated with 650 nm light at a fluence of 10 J/cm^2 at an irradiance of 42.1 mW/cm^2. Twenty-four hours after the light treatment, tumors were excised, sectioned and stained for apoptosis. TUNEL staining clearly indicated severe apoptosis in large areas of tumor. In addition, significant tissue loss was observed in the L-SR15 treated group. In contrast, the D-SR16 injected and light treated tumor showed no signs of apoptosis.

Antitumor efficacy was further evaluated by measuring tumor growth rates. When tumors reached 3-5 mm, mice were divided into 5 groups. Animals were treated with L-SR15 with light illumination, D-SR16 with light illumination, L-SR15 without light

illumination, free Ce6 with illumination or PBS with light illumination. In the group received L-SR15 with light illumination the mean tumor volume was 46% at day 6 (P=0.0067) and 54% at day 9 (P=0.0249) compared to control groups. All other treated groups, including L-SR15 without light, free Ce6 with light and PBS with light treated groups, showed no significant antitumor effects. Only the combination of protease degradable L-SR15 and light illumination resulted in reduced tumor growth rates. These data support the hypothesis that tumor-associated proteases can activate the proposed anti-cancer agents in tumor.

Key research accomplishments

- Synthesize a cathepsin B activatable anticancer agent
- In vitro confirmation of its biological properties
- In vivo demonstration of anti-cancer effect

Reportable outcomes:

Publication:

1. Choi Y, Weissleder R, Tung CH. Selective anti-tumor effect of novel protease-mediated photodynamic agent. Cancer Res, 2006, 66, 7225-7229.
2. Choi Y, Weissleder R, Tung CH. Protease-mediated phototoxicity of polylysine-chlorin$_{e6}$ conjugate. ChemMedChem, 2006, 1, 698-701.
3. Choi Y, McCarthy J, Weissleder R, Tung CH. Conjugation of a photosensitizer to an oligoarginine-based cell penetrating peptide increases the efficacy of photodynamic therapy. ChemMedChem, 2006, 1, 458-463.

Abstracts:

1. Tung CH. Fluorescent chemistries: next generation of optical reagents [Abstract] Imaging in 2020, Jackson Hole, WY, 9/2005.
2. Tung CH. Next wave of medical imaging-molecular imaging [Abstract] Radiology Society, Kaohsiung, Taiwan, 3/2006.
3. Choi Y, Weissleder R, Tung CH. Protease-mediated near-infrared fluorescence tumor imaging and therapy. [Abstract] Society for Molecular Imaging, Hawaii, 9/2006.

Presentation

1. Mechanistic basis of optical molecular imaging probes. Molecular Imaging Program, Stanford School of Medicine, Stanford, CA, 1/2006.
2. Enzyme mediated molecular imaging and photomedicine. Wellman Photomedicine Center, Massachusetts General Hospital, Harvard Medical School, Boston, MA, 3/2006.
3. Next wave of medical imaging-molecular imaging. Radiology Society, Kaohsiung, Taiwan, 3/2006.
4. Proteases and drug development. Institute of Biotechnology, Kaohsiung Medical University, Kaohsiung, Taiwan, 3/2006.
5. Managing diseases using fluorescence lights. Department of Clinical Medicine, VA Hospital, Taipei, Taiwan, 3/2006.
6. Imaging proteases during therapeutic treatments. Gordon Conference on Proteolytic Enzymes and Their Inhibitors. New London, NH, 7/2006.

Conclusion:

Prolonged administration of effective concentrations of conventional photosensitizers is usually not possible because of dose-limiting systemic phototoxicities (limited therapeutic window). The combination of the presented protease mediated anticancer therapy and focal light illumination is expected to be an effective treatment with reduced phototoxicity given the quenched state of the native compounds. We show in this study that SOG can be quenched and activated through proteolytic cleavage. Since activation of presented protease mediated anticancer therapeutic agents is largely confined to areas of cancer, most unwanted side effects could be prevented. Potentially, the proposed presented protease mediated anticancer therapy could be used as a primary anti-cancer treatment or as an adjuvant to other therapeutic options. Although its treatment effect is restricted by the limited tissue penetration of light, PDT remains a promising therapy to treat various superficial cancers, e.g., breast, esophagus, gastric, colon, and cervical cancers. Importantly, the proposed strategy is one of the few that allows visualization of the target and local drug concentration prior to selective therapy. This therapeutic approach could be used to tailor treatments and avoid unnecessary side effects. We believe that the reported protease mediated anticancer therapy has significant translational potential.

Appendices

1. Choi Y, Weissleder R, Tung CH. Selective anti-tumor effect of novel protease-mediated photodynamic agent. Cancer Res, 2006, 66, 7225-7229.
2. Choi Y, Weissleder R, Tung CH. Protease-mediated phototoxicity of polylysine-chlorin$_{e6}$ conjugate. ChemMedChem, 2006, 1, 698-701.
3. Choi Y, McCarthy J, Weissleder R, Tung CH. Conjugation of a photosensitizer to an oligoarginine-based cell penetrating peptide increases the efficacy of photodynamic therapy. ChemMedChem, 2006, 1, 458-463.

Selective Antitumor Effect of Novel Protease-Mediated Photodynamic Agent

Yongdoo Choi, Ralph Weissleder, and Ching-Hsuan Tung

Center for Molecular Imaging Research, Massachusetts General Hospital, Harvard Medical School, Charlestown, Massachusetts

Abstract

A new approach to selective photodynamic therapy (PDT) was developed by designing chlorin e6 (Ce6)–containing macromolecules, which are sensitive to tumor-associated proteases. The agents are nontoxic in their native state but become fluorescent and produce singlet oxygen on protease conversion. Coupled with optimized delivery systems, we show that (*a*) the agents efficiently accumulate in tumors due to the enhanced permeability and retention effect, (*b*) the agents are locally activated by proteases, (*c*) local drug concentrations can be measured by quantitative fluorescence tomography, and (*d*) light-treated tumors show reduced growth. A single low dose of PDT (0.125 mg Ce6 equivalent/kg) was sufficient to suppress tumor growth by >50%. Activatable singlet oxygen generation agents provide increased efficacy with reduced toxicity, and it could become a powerful PDT. (Cancer Res 2006; 66(14): 7225-9)

Introduction

Photodynamic therapy (PDT) using combinations of chemical photosensitizers and light has been used successfully to treat cancers and other nonmalignant conditions (1). Typical photosensitizers are designed to be nontoxic to cells in the absence of light. When illuminated by an appropriate wavelength, the excited photosensitizer transfers its energy to neighboring molecular oxygen, producing cytotoxic singlet oxygen, which causes selective damage to tissues *in situ*. Despite significant advantages of PDT over the conventional chemotherapy, limited tumor selectivity of PDT agents has remained major obstacles. In addition, phototoxicity to skin and eyes is a considerable limitation of existing agents (1). In the current study, we developed a new strategy termed protease-mediated PDT (PM-PDT). This was achieved by constructing PDT agents that are "activatable" by tumor-associated proteases.

Tumor-associated proteases are known to function at multiple stages of tumor progression, affecting tumor establishment, growth, neovascularization, intravasation, extravasation, and metastasis (2–5). Prior reports have shown that several proteases (e.g., cathepsins and matrix metalloproteinases) are up-regulated in many cancer types (6–8), and potentially, these tumor-associated proteases could act as activators of the proposed PM-PDT agent.

Porphyrin-based photosensitizers have been shown previously to exhibit reduced fluorescence and singlet oxygen generation (SOG) on aggregation (9–11). Based on this observation, we coupled multiple chlorin e6 (Ce6) molecules onto a biodegradable poly-L-lysine grafted with monomethoxy-polyethylene glycol (PEG; L-PGC) to induce aggregation and self-quenching (Fig. 1) while still representing a biocompatible agent with favorable tumor-accumulating properties (12). Previously, we have used analogous backbones to synthesize protease activatable imaging probes (13). We hypothesized that the high local density of Ce6 causes quenching (i.e., low fluorescence and low SOG). Fluorescence and SOG are expected to increase on protease-mediated release of the photosensitizers.

Materials and Methods

Synthesis of L-SR15 and D-SR16. L-PGC (average molecular weight, 375 kDa) and D-PGC (average molecular weight, 344 kDa) were purchased from VisEn Medical, Inc. (Woburn, MA). L-PGC consists of poly-L-lysine (48 kDa) backbone grafted with monomethoxy-PEG (5 kDa, percent PEGylation, 30%). D-PGC consists of poly-D-lysine (44 kDa) grafted with PEG (percent PEGylation, 28%). The conjugation of Ce6 (Frontier Scientific, Logan, UT) to lysine residues in the PGC backbone was done using 1-ethyl-3-(3-dimethylaminopropyl)carbodiimide HCl (EDC) as a coupling agent. In brief, total 1.7 mL mixture solutions, consisting of 1,140 μL of 9 μmol/L L-PGC or D-PGC in distilled water, 423 μL of 1.8 mmol/L Ce6 in 33 mmol/L Na_2HPO_4, and 120 μL of 13 mmol/L EDC in distilled water, were added into microcentrifuge tubes and gently shaken at 25°C in the dark for 20 hours. After reaction, the conjugates were purified by size exclusion chromatography (Bio-Gel P-10 gel, Bio-Rad, Hercules, CA) using 10 mmol/L phosphate buffer (pH 7.4) as an eluent. The substitution ratio of Ce6 on each PGC chains was determined by measuring the absorbance at 400 nm of conjugates dissolved in 0.1 mol/L NaOH/0.1% SDS and calculating the amount of Ce6 present using ε_{400nm} = 150,000 (11). The substitution ratio (i.e., the number of Ce6 attached to each PGC chain) was 15 for L-PGC conjugate (L-SR15) and 16 for D-PGC conjugate (D-SR16), respectively.

Enzyme activation of fluorescence signal and SOG. Enzymatic activation of the conjugates by cathepsin B was tested as following: L-SR15 or D-SR16 (0.84 nmol Ce6 eq.) dissolved in 34 μL sodium acetate buffer [20 mmol/L sodium acetate, 1 mmol/L EDTA, 1 mmol/L DTT (pH 5.0)] was mixed with 0.2 nmol cathepsin B (8 μL in sodium acetate buffer, human liver, Calbiochem, La Jolla, CA) for the enzyme-treated sample or equal volume of sodium acetate buffer (8 μL) for the buffer-treated sample. The mixture was then incubated at 37°C for 22 hours. To compare enzymatic cleavage of L-SR15 conjugate by cathepsins, identical molar amounts of cathepsin L (human liver, Calbiochem) or cathepsin S (human spleen, Calbiochem) were incubated with the conjugate using identical conditions as described above.

For samples treated with a specific cathepsin B inhibitor CA-074 (Peptide International, Louisville, KY), 0.2 nmol cathepsin B (8 μL) was incubated with 1 mmol/L CA-074 (8 μL) in 20 mmol/L sodium acetate buffer (pH 5.0) at room temperature for 10 minutes. Then, L-SR15 or D-SR16 (0.8 nmol Ce6 eq.) dissolved in 26 μL sodium acetate buffer [20 mmol/L sodium acetate, 1 mmol/L EDTA, 1 mmol/L DTT (pH 5.0)] was added into CA-074-pretreated cathepsin B solution and incubated at 37°C for 22 hours. Before measuring fluorescence intensities of the samples, 160 μL phosphate buffer [10 mmol/L phosphate, 140 mmol/L NaCl, 3 mmol/L KCl (pH 7.4)] was

Requests for reprints: Ching-Hsuan Tung, Center for Molecular Imaging Research, Massachusetts General Hospital, Harvard Medical School, 149, 13th Street, Room 5406, Charlestown, MA 02129. Phone: 617-726-5779; Fax: 617-726-5708; E-mail: tung@helix.mgh.harvard.edu.

doi:10.1158/0008-5472.CAN-06-0448

added to each sample. Thereafter, emission (excitation, 650 nm) was recorded at 670 nm using a computer-controlled fluorescence plate reader (Safire II, Tecan, Durham, NC).

Bleaching of *N,N*-dimethyl-4-nitrosoaniline (RNO) was used as an indicator for photo-induced singlet oxygen in the presence of histidine as a chemical trap for singlet oxygen (14). In brief, the sample solution used in the fluorescence measurement was prepared by mixing 480 μL RNO solution [20 mmol/L phosphate, 20 mmol/L histidine, 100 μmol/L RNO (pH 7.0)]. The mixture was added into a UV quartz cell and irradiated with light at a dose rate of 41.4 mW/cm^2 at 650 nm. At 0 minute and every 2 minutes of light treatment, solutions were mixed by pipetting and transferred to the UV spectrophotometer. The bleaching of RNO was measured at 440 nm. SOG was calculated from the initial slope of the RNO variation versus irradiation time. SOG of free Ce6 was measured at the same condition, which was used for the conjugates. Relative values of SOG of the conjugates compared with free Ce6 equal to the slope of unknown samples divided by the mean slope of free Ce6. All experiments were done in triplicate.

***In vivo* PDT.** All animal studies were approved by the Institutional Animal Care Committee. HT1080 (human fibrosarcoma) obtained from American Type Culture Collection (Manassas, VA) were maintained in DMEM (Cellgro, Washington, DC) supplemented with 10% fetal bovine serum (Cellgro) and 1% penicillin/streptomycin at 37°C in humidified atmosphere with 5% CO_2. Female athymic nude mice (*nu/nu*, 6-7 weeks old, 21-23 g) were purchased from Charles River (Wilmington, MA). HT1080 cell line (1.5×10^6 cells/0.05 mL DMEM) was implanted s.c. into both hind legs of each mouse. When the tumors reached 3 to 5 mm in diameter, a total of 70 healthy mice (8 mice for fluorescence imaging, 15 mice for apoptosis study, and 47 mice for tumor growth) were randomly divided into five groups. L-SR15 or D-SR16 was dissolved in sterilized PBS [10 mmol/L, 140 mmol/L NaCl, 3 mmol/L KCl (pH 7.4)] at a concentration of 35.7 μmol/L, respectively. Mice in groups 1 and 2 received i.v. injection of either L-SR15 (group 1, 16 mice) or D-SR16 (group 2, 16 mice) at the dose of 0.125 mg Ce6 equivalent/kg. One day after drug injection, mice were treated with light using a diode laser at 650 nm to give dose of 10 J/cm^2 at an irradiance of 42 mW/cm^2, and light spot diameter was 1 cm. Eight mice in group 3 received i.v. injection of L-SR15 at the same dose but were not treated with light. Mice in groups 4 and 5 received i.v. injection of either free Ce6 (0.125 mg/kg, 15 mice in group 4) or sterilized PBS (140 μL/mouse, 15 mice in group 5) followed by light treatment at 24 hours postinjection.

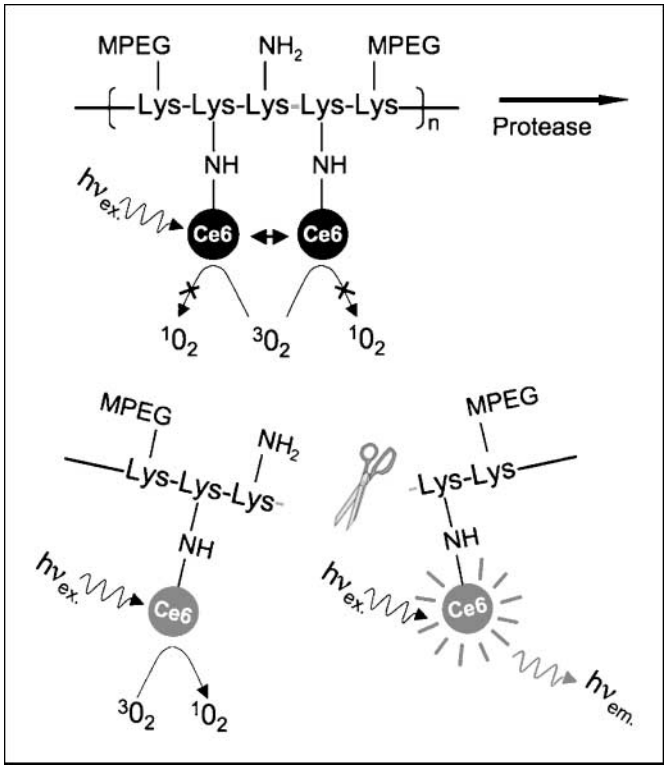

Figure 1. Schematic diagram of PM-PDT strategy. Fluorescence and SOG is quenched due to energy transfer between Ce6 molecules. Following proteolytic cleavage of the peptide backbone, released Ce6 regains its fluorescent properties and SOG on light excitation.

The day of photosensitizer injection was considered as day 0 and tumor volumes of the mice were measured periodically at days 0, 1, 4, 6, and 9. Tumor volume was calculated using the formula: 1/2 × length × width × height (15). To observe the enzymatic activation of L-SR15 in tumor tissues, tumors from eight mice were collected by sampling two mice from each of the groups 1, 2, 4, and 5 after 24 hours of i.v. injection of buffer or PGC conjugate solution. These mice did not receive light treatment. Collected tumors were snap frozen in liquid nitrogen, cut into 7 μm sections, air-dried, and mounted on slides. Mounting medium (Vectashield, Vector Laboratories, Burlingame, CA) with 4′,6-diamidino-2-phenylindole (DAPI) was used to counter stain nuclei of the tumor sections. Sections were viewed by fluorescence microscopy (Nikon Eclipse 80i, Nikon, Melville, NY).

To investigate tissue damage after PDT, tumor tissues from 15 mice were collected by sampling 3 mice from each of the groups 1 to 5 at 24 hours after PDT. Tumors were snap frozen in liquid nitrogen, cut into 7 μm sections, air-dried, and stained using the terminal deoxynucleotidyl transferase–mediated dUTP nick end labeling (TUNEL) technique with the ApopTag kit (Chemicon, Temecula, CA). Normal or apoptotic nuclei were stained as green or brown, respectively.

Fluorescence molecular tomography. Fluorescence molecular tomography (FMT) experiments were done using a commercially available imaging system (FMT-Solaris; VisEn Medical). Three mice (total of six tumors) were used for FMT imaging. These mice received i.v. injection of L-SR15 (0.125 mg Ce6 eq./kg) and were imaged at 24 hours postinjection. The images were acquired with 680 nm excitation laser and 715 nm emission (bandwidth, 30 nm). Briefly, objects were positioned in the imaging chamber and surrounded by matching fluid composed of 1% Intralipid (Fresenius, Melsungen, Germany) and 0.5% ink, which closely matched the optical properties of tissues. During FMT image acquisition, only the lower half of the mouse was imagined. Following data reconstruction of the entire field of view, regions of interest are selected in all three planes of view (*X, Y, Z*) and a volume of interest is generated. Image data sets were reconstructed using a normalized Born forward model adapted to small mouse models (16, 17). Details of the algorithm have been published before (17). Image acquisition time per animal was 3 to 5 minutes and reconstruction time was 1 to 3 minutes. Images were displayed as raw data sets (excitation, emission, and masks) and as reconstructed three-dimensional data sets in axial, sagittal, and coronal planes. Fluorochrome concentration in the target was automatically calculated from reconstructed images and expressed as femtomole fluorochrome/defined target volume.

Statistical analysis. Mean ± SD values were used for the expression of data if there is no mention about that. Statistical analyses of data were done using Student's *t* test. Differences of $P < 0.05$ were considered statistically significant.

Results and Discussion

Following initial optimization experiments, a preparation with 15 Ce6 molecules per L-PGC molecule (L-SR15) was chosen for subsequent studies. L-SR15 showed an 86% decrease in fluorescence compared with that of free Ce6. L-PGC is a known substrate for cysteine protease (12); therefore, L-SR15 was tested against several cysteine proteases, including cathepsins B, L, and S, at pH 5.0. Among these three proteases, cathepsin B induced the highest fluorescence (Fig. 2*A*). L-SR15 treated with cathepsin B or L showed 4.0 ($P = 0.0007$) or 1.6 ($P = 0.0012$) times higher fluorescence intensities compared with control (buffer-treated L-SR15).

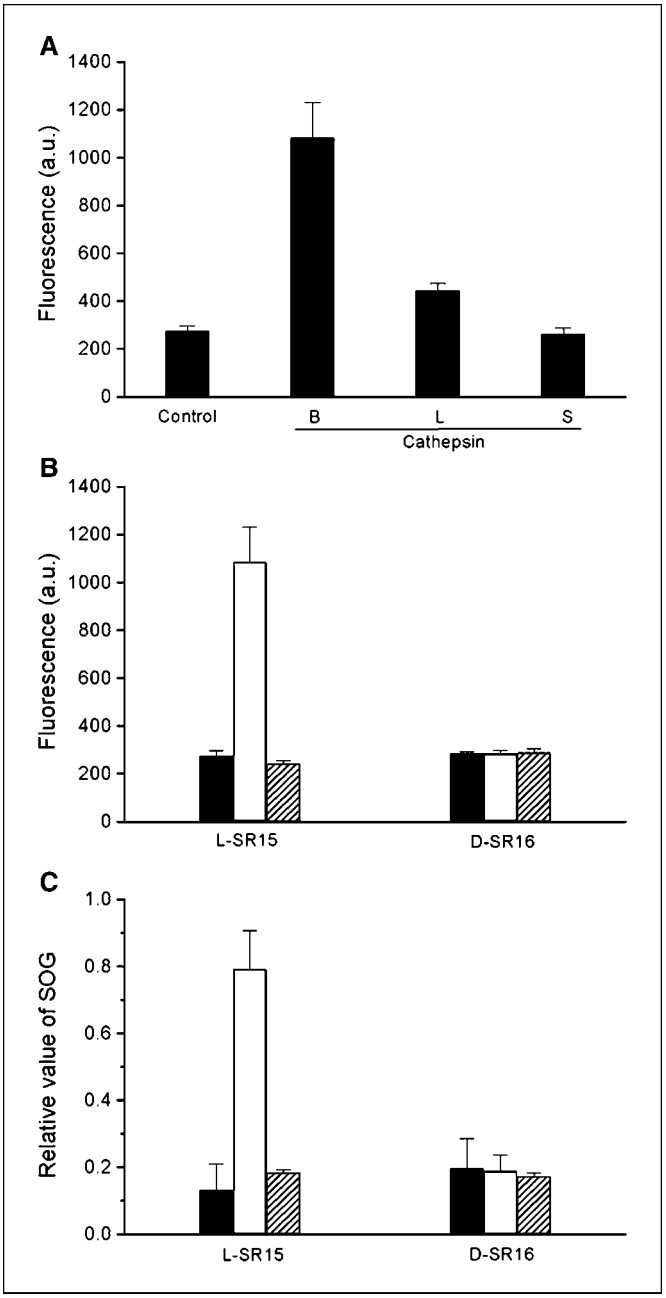

Figure 2. Fluorescence activation and single oxygen generation on protease treatment. *A,* fluorescence intensity changes of L-SR15 following treatment with phosphate buffer, cathepsin B, cathepsin L, or cathepsin S. Activation of fluorescence intensity (*B*) and SOG (*C*) of L-SR15 and D-SR16 with phosphate buffer (*black columns*), cathepsin B (*white columns*), and CA-074 inhibitor-pretreated cathepsin B (*striped columns*).

Several experiments were subsequently conducted to corroborate specificity. The cathepsin B inhibitor CA-074 (18) completely inhibited fluorescence recovery on cathepsin B addition (Fig. 2*B*). Furthermore, a poly-D-lysine-based PGC with similar substitution ratio (D-SR16) was also prepared and tested under identical conditions. Similar fluorescence quenching effect (~86% quenching) was observed with the D-backbone; however, no noticeable fluorescence activation occurred on cathepsin B addition. The above results thus confirm that proteolytic degradation is indeed the primary mechanism of fluorescence activation.

SOG of L-SR15 and D-SR16 was subsequently assayed using similar cathepsin B incubation experiments (Fig. 2*C*). In the native state, SOG of L-SR15 was only 13% compared with that of free Ce6 at equimolar concentrations. In the absence of cathepsin B, the buffer containing L-SR15 remained quenched. On cathepsin B treatment, SOG increased up to 79%, a 6-fold increase ($P = 0.0012$). As with the fluorescence experiment, inhibitory effects were observed with CA-074 treatment. As expected, addition of cathepsin B to D-SR16 showed no enhancement in SOG. These results support the hypothesis that not only fluorescence but also SOG can be quenched and selectively recovered on specific protease treatments.

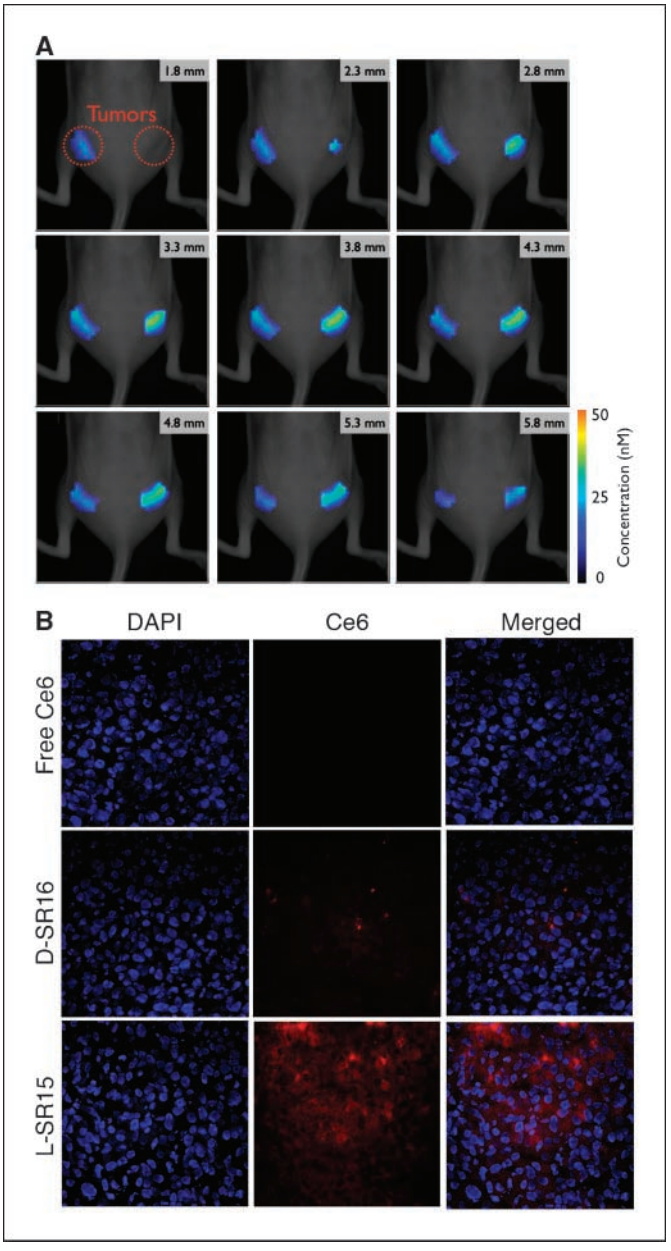

Figure 3. *In vivo* activation of PM-PDT. *A,* distribution of imageable Ce6 in bilateral flank tumors. Nine consecutive slices from a three-dimensional fluorescence-mediated tomographic scan. *B,* tumor-bearing mice were injected with free Ce6, D-SR16, or L-SR15. Twenty-four hours later, tumors were collected without light treatment. *Left,* nuclear DAPI staining (*blue*); *middle,* fluorescent signal of Ce6 (*red*); *right,* merged images. Magnification, ×40.

The PM-PDT strategy was next examined *in vivo* using a xenographic tumor model. HT1080 cell line was selected for the animal study because of its high-expressing level of cathepsin B (19). HT1080 human fibrosarcomas were s.c. implanted in both hind legs of mice. After i.v. injection of L-SR15 (0.125 mg Ce6 eq./kg), the fluorescence activation in tumors (n = 6) were clearly imaged using FMT. There was accumulation of L-SR15 in tumor with time, reaching the highest concentration of 17.0 ± 1 nmol/L at 24 hours postinjection (Fig. 3*A*). In a separate set of animals, free Ce6, L-SR15, or D-SR16 (0.125 mg Ce6 eq./kg) was injected i.v.; tumors were collected and sectioned. These animals received no light treatment to preserve fluorescence signal. High fluorescence signal was observed in the animals injected with L-SR15, whereas D-SR16- and Ce6-injected groups showed little or no fluorescence signal (Fig. 3*B*). These results support that L-SR15 is activated in tumors *in vivo* similar as in the previous *in vitro* assays. Merged images showed that the fluorescence of L-SR15 fragments was distributed in cellular cytoplasm but did not localize to the nucleus. On the contrary, D-SR16-treated animals did not show any significant fluorescence in tumors. Although cathepsin B is known as a lysosomal enzyme, it also locates on the surface of cancer cells (20). It explains how the injected L-SR15 conjugate can be efficiently activated in tumors. Another interesting finding was that fluorescence signal of free Ce6 was much lower than that of L-SR15-injected animals. Polymeric drug carriers with PEG grafting, such as PGC conjugate, have shown prolonged blood circulation and higher accumulation in tumors by the EPR effect (12, 21, 22).

To show therapeutic efficacy *in vivo*, L-SR15 or D-SR16 (0.125 mg Ce6 eq./kg) in PBS was injected i.v., and 24 hours later, animals were treated with 650 nm light at a fluence of 10 J/cm^2 at an irradiance of 42.1 mW/cm^2. Twenty-four hours after the light treatment, tumors were excised, sectioned, and stained for apoptosis. TUNEL staining clearly indicated severe apoptosis in large areas of tumor (Fig. 4*A*). In addition, significant tissue loss was observed in the L-SR15-treated group. In the destructed area, polymorphonuclear cells were also observed, indicating inflammatory responses. In contrast, the D-SR16-injected and light-treated tumor showed no signs of apoptosis (Fig. 4*B*).

Antitumor efficacy of PM-PDT was further evaluated by measuring tumor growth rates. When tumors reached 3 to 5 mm, mice were divided into five groups. Animals were treated with L-SR15 with light illumination (group 1), D-SR16 with light illumination (group 2), L-SR15 without light illumination (group 3), free Ce6 with illumination (group 4), or PBS with light illumination (group 5). In the group that received L-SR15 with light illumination, the mean tumor volume was 46% at day 6 (P = 0.0067) and 54% at day 9 (P = 0.0249) compared with group 2 (Fig. 4*C*). All other treated groups, including L-SR15 without light, free Ce6 with light, and PBS with light, showed no significant antitumor effects. Only the combination of protease-degradable L-SR15 and light illumination resulted in reduced tumor growth rates (Fig. 4*D* and *E*). These data support the hypothesis that tumor-associated proteases can activate PM-PDT agents in tumor.

Prolonged administration of effective concentrations of conventional photosensitizers is usually not possible because of dose-limiting systemic phototoxicities (limited therapeutic window). The combination of the presented PM-PDT and focal light illumination is expected to be an effective treatment with reduced phototoxicity given the quenched state of the native compounds. We show in this study that SOG can be quenched and activated through proteolytic cleavage. Because activation of PM-PDT agents is largely confined to areas of cancer, most unwanted side effects could be prevented. Potentially, the proposed PM-PDT approach could be used as a primary anticancer treatment or as an adjuvant to other therapeutic options. Although its treatment effect is restricted by the limited tissue penetration of light, PDT remains a promising therapy to treat various superficial cancers (e.g., esophageal, gastric, colon, and cervical cancers). Importantly, the proposed strategy is one of the few that allows visualization of the target and local drug concentration before selective therapy (Fig. 3). This therapeutic approach could be used to tailor treatments and avoid unnecessary side effects. We believe that the reported PM-PDT has significant translational potential.

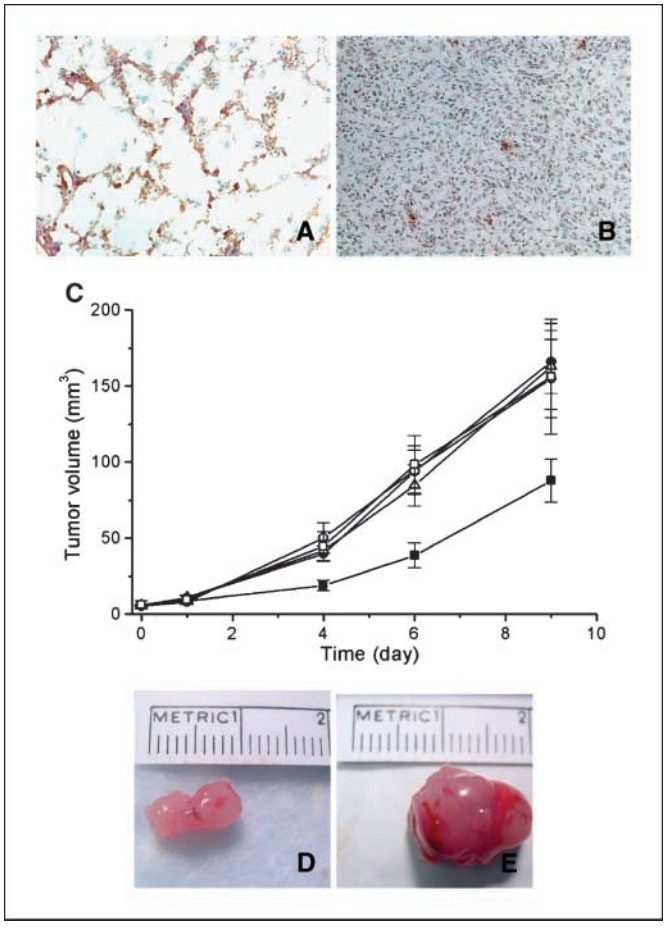

Figure 4. *In vivo* PDT. TUNEL staining of (*A*) L-SR15-treated or (*B*) D-SR16-treated tumors 24 hours after light illumination. Magnification, ×20. A 24-hour lag time was applied to allow *in vivo* proteases activation. *C,* tumor size after PM-PDT treatment. *Points,* mean; *bars,* SE. ●, PBS + light illumination (n = 17); ○, free Ce6 + illumination (n = 18); △, D-SR16 + illumination (n = 20); □, L-SR15 without illumination (n = 8); ■, L-SR15 + illumination (n = 19). n = number of tumors involved. *D,* tumor treated with L-SR15 + light. *E,* tumor treated with D-SR16 + light.

Acknowledgments

Received 2/6/2006; revised 4/12/2006; accepted 5/11/2006.

Grant support: NIH grants P50-CA86355, RO1 CA99385, and DOD DC044945.

The costs of publication of this article were defrayed in part by the payment of page charges. This article must therefore be hereby marked *advertisement* in accordance with 18 U.S.C. Section 1734 solely to indicate this fact.

We thank Peter Waterman for the FMT imaging.

References

1. MacDonald IJ, Dougherty TJ. Basic principles of photodynamic therapy. J Porphyrins Phthalocyanines 2001;5:105–29.
2. Keppler D, Sameni M, Moin K, Mikkelsen T, Diglio CA, Sloane BF. Tumor progression and angiogenesis: cathepsin B & Co. Biochem Cell Biol 1996;74:799–810.
3. Kim J, Yu W, Kovalski K, Ossowski L. Requirement for specific proteases in cancer cell intravasation as revealed by a novel semiquantitative PCR-based assay. Cell 1998;94:353–62.
4. Liaudet E, Derocq D, Rochefort H, Garcia M. Transfected cathepsin D stimulates high density cancer cell growth by inactivating secreted growth inhibitors. Cell Growth Differ 1995;6:1045–52.
5. Garcia M, Platet N, Liaudet E, et al. Biological and clinical significance of cathepsin D in breast cancer metastasis. Stem Cells 1996;14:642–50.
6. DeClerck YA, Mercurio AM, Stack MS, et al. Proteases, extracellular matrix, and cancer: a workshop of the path B study section. Am J Pathol 2004;164:1131–9.
7. Koblinski JE, Ahram M, Sloane BF. Unraveling the role of proteases in cancer. Clin Chim Acta 2000;291:113–35.
8. Lynch CC, Matrisian LM. Matrix metalloproteinases in tumor-host cell communication. Differentiation 2002;70:561–73.
9. Redmond RW, Land EJ, Truscott TG. Aggregation effects on the photophysical properties of porphyrins in relation to mechanisms involved in photodynamic therapy. Adv Exp Med Biol 1985;193:293–302.
10. Damoiseau X, Schuitmaker HJ, Lagerberg JW, Hoebeke M. Increase of the photosensitizing efficiency of the Bacteriochlorin a by liposome-incorporation. J Photochem Photobiol B 2001;60:50–60.
11. Hamblin MR, Miller JL, Rizvi I, Ortel B. Degree of substitution of chlorin e6 on charged poly-L-lysine chains affects their cellular uptake, localization and phototoxicity towards macrophages and cancer cells. J X-Ray Sci Technol 2002;10:139–52.
12. Weissleder R, Tung CH, Mahmood U, Bogdanov A, Jr. *In vivo* imaging of tumors with protease-activated near-infrared fluorescent probes. Nat Biotechnol 1999;17:375–8.
13. Tung CH. Fluorescent peptide probes for *in vivo* diagnostic imaging. Biopolymers 2004;76:391–403.
14. Hartman PE, Hartman Z, Ault KT. Scavenging of singlet molecular oxygen by imidazole compounds: high and sustained activities of carboxy terminal histidine dipeptides and exceptional activity of imidazole-4-acetic acid. Photochem Photobiol 1990;51:59–66.
15. Tomayko MM, Reynolds CP. Determination of subcutaneous tumor size in athymic (nude) mice. Cancer Chemother Pharmacol 1989;24:148–54.
16. Ntziachristos V, Schellenberger EA, Ripoll J, et al. Visualization of antitumor treatment by means of fluorescence molecular tomography with an Annexin V-Cy5.5 conjugate. Proc Natl Acad Sci U S A 2004;101:12294–9.
17. Graves EE, Weissleder R, Ntziachristos V. Fluorescence molecular imaging of small animal tumor models. Curr Mol Med 2004;4:419–30.
18. Yamamoto A, Kaji T, Tomoo K, et al. Crystallization and preliminary X-ray study of the cathepsin B complexed with CA074, a selective inhibitor. J Mol Biol 1992;227:942–4.
19. Hulkower KI, Butler CC, Linebaugh BE, et al. Fluorescent microplate assay for cancer cell-associated cathepsin B. Eur J Biochem 2000;267:4165–70.
20. Cavallo-Medved D, Sloane BF. Cell-surface cathepsin B: understanding its functional significance. Curr Top Dev Biol 2003;54:313–41.
21. Bogdanov AA, Jr., Martin C, Bogdanova AV, Brady TJ, Weissleder R. An adduct of *cis*-diamminedichloroplatinum(II) and poly(ethylene glycol)poly(L-lysine)-succinate: synthesis and cytotoxic properties. Bioconjug Chem 1996;7:144–9.
22. Satchi-Fainaro R, Puder M, Davies JW, et al. Targeting angiogenesis with a conjugate of HPMA copolymer and TNP-470. Nat Med 2004;10:255–61.

DOI: 10.1002/cmdc.200600053

Protease-Mediated Phototoxicity of a Polylysine–Chlorin$_{e6}$ Conjugate

Yongdoo Choi, Ralph Weissleder, and Ching-Hsuan Tung*[a]

Type II photosensitizers generate cytotoxic singlet oxygen ($^1O_2$) by energy transfer from the triplet excited state to neighboring oxygen molecules.[1] Owing to this action, target tissues such as tumors can be selectively destroyed by local illumination following intravenous administration of a photosensitizer. Although many photosensitizers accumulate to some degree in tumors, they also distribute to normal tissues and show undesired phototoxicity such as skin photosensitivity brought on by bright indoor light or sunlight.[2] Thus, it is recommended that patients avoid exposure to sunlight for several weeks to months following photodynamic therapy (PDT). Herein, we report a novel design of protease-mediated photosensitization by which phototoxicity can be selectively turned on through tumor-associated proteases (Figure 1a). As normal tissues exhibit highly regulated protease expression, phototoxicity in normal tissues can be minimized.

To obtain convertible phototoxicity, multiple copies of the photosensitizer chlorin$_{e6}$ (Ce6), were conjugated onto a poly-L-lysine backbone, similar to previously developed protease-activated near-infrared (NIR) fluorescent probes for cancer imaging.[3] Ce6, a commercially available second-generation photosensitizer, was chosen for conjugation because of its reactivity and the significant overlap between its emission and absorption spectra (Figure 1b). The overlapping spectra and close geometry between the conjugated photosensitizers make self-quenching efficient,[4] thereby prohibiting the process of energy transfer between the photosensitizer and neighboring oxygen, and thus inhibiting the generation of cytotoxic singlet oxygen. When the peptide linkages of the polylysine backbone are cleaved by tumor-associated enzymes (such as cathepsins), the degraded probes become highly phototoxic and fluorescent because no more resonance energy transfer occurs between the photosensitizers. A second possibility for the induction of the self-quenching is the formation of intramolecular aggregates of the conjugated photosensitizers. Porphyrin-based photosensitizers have been shown to have decreased fluorescence intensity upon aggregation at increased concentrations. The decrease in fluorescence intensity is directly proportional to the decrease in the production of triplet state intermediates and singlet oxygen.[5–7] Based on these observations, we hypothesized that conjugation of multiple Ce6 molecules onto a polymer backbone would induce aggregation of the conjugated Ce6 depending on the conjugation ratio within the polymer backbone, resulting in diminished fluorescence and singlet oxygen generation.

Ce6 was conjugated to poly-L-lysine grafted with monomethoxy-poly(ethylene glycol) (L-PGC) at various ratios (Supporting Information). To optimize the quenching-to-activation ratio, four substitution ratios (SR) of the L-PGC conjugate were prepared: 0.9 ± 0.7, 5.9 ± 0.1, 15.0 ± 1.2, and 36.4 ± 0.8 Ce6 molecules per L-PGC chain, referred to as L-SR1, L-SR6, L-SR15, and L-SR36, respectively. The same polymeric template, but with non-natural D-lysine residues (D-PGC), was used as a control for Ce6 conjugation because the D-form polypeptide is not readily degraded by natural proteases. Three similar substitution ratios of D-PGC conjugate were prepared with 4.3 ± 0.3, 16.2 ± 0.6, and 39.8 ± 0.5 Ce6 molecules per D-PGC chain (D-SR4, D-SR16, and D-SR40, respectively).

The fluorescence properties of the conjugates were compared at an equimolar concentration of Ce6 in phosphate buffer solution (10 mM, pH 7.0). It was found that the fluorescence intensity of the conjugates decreased with increasing substitution ratios of Ce6 (Figure 2a). When the L-PGC conjugates were digested by the lysine-recognizing protease trypsin, fluorescence intensities were increased twofold for L-SR6 and L-SR36, and 4.2-fold for L-SR15. No change in the fluorescence intensity was observed for L-SR1, indicating that there was no quenching in the native state. In contrast, D-PGC conjugates also showed SR-dependant fluorescence quenching, but there was no significant fluorescence change following protease treatment (Figure 2b).

Singlet oxygen generation (SOG) of the conjugates showed trends similar to the fluorescence properties discussed above (Figure 2c and d). SOG of both L- and D-PGC conjugates decreased with increasing SR of Ce6. The SOG of L-SR6 was 32% of that of free Ce6 at equimolar concentrations, and that of L-SR15 was further decreased to 12%. No SOG was observed with L-SR36. Similar trends were observed for D-PGC conjugates. Importantly, SOG was recovered by proteolysis. Treatment of the conjugates L-SR6 and L-SR15 with trypsin resulted in 2.7 and 5.4-fold increases in SOG, which represent 86 and 65% recovery of total phototoxicity, respectively (Figure 2c). As observed in fluorescence activation experiments, no improvement in SOG was observed with L-SR36. None of the D-PGC conjugates showed changes in SOG with enzyme treatment, as their peptide backbones are nondegradable (Figure 2d).

Comparison of the UV/Vis absorption spectra of L-SR15, L-SR36, and free Ce6 in phosphate buffer solution indicates the presence of aggregation after conjugation, as shown in Figure 3a and b.[8,9] Both conjugates showed significant broadening of the Soret band region of the spectrum, whereas L-SR36 showed a broader spectrum than that of L-SR15. Following trypsin treatment for 4 h, the absorption spectrum of L-SR15 narrowed and approximated the spectrum of free Ce6 (Figure 3a). In contrast, L-SR36 still showed minor changes in the UV/Vis spectrum following trypsin treatment (Figure 3b). By in-

[a] Dr. Y. Choi, Prof. Dr. R. Weissleder, Prof. Dr. C.-H. Tung
Center for Molecular Imaging Research
Massachusetts General Hospital
149 13th Street, Room 5406
Charlestown, Massachusetts 02129 (USA)
Fax: (+1) 617-726-5708
E-mail: tung@helix.mgh.harvard.edu

Supporting information for this article is available on the WWW under http://www.chemmedchem.org or from the author.

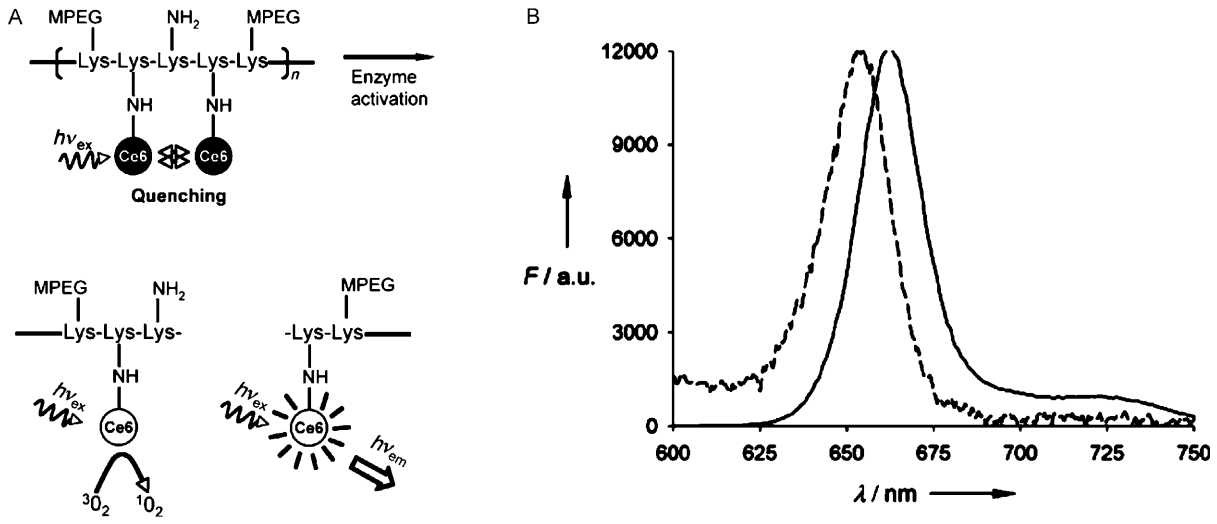

Figure 1. A) Activation of fluorescence signal and generation of singlet oxygen by protease activity; B) absorption (-----) and emission (——) ($\lambda_{ex}=400$ nm) profiles of Ce6 in phosphate buffer (10 mM, pH 7.4).

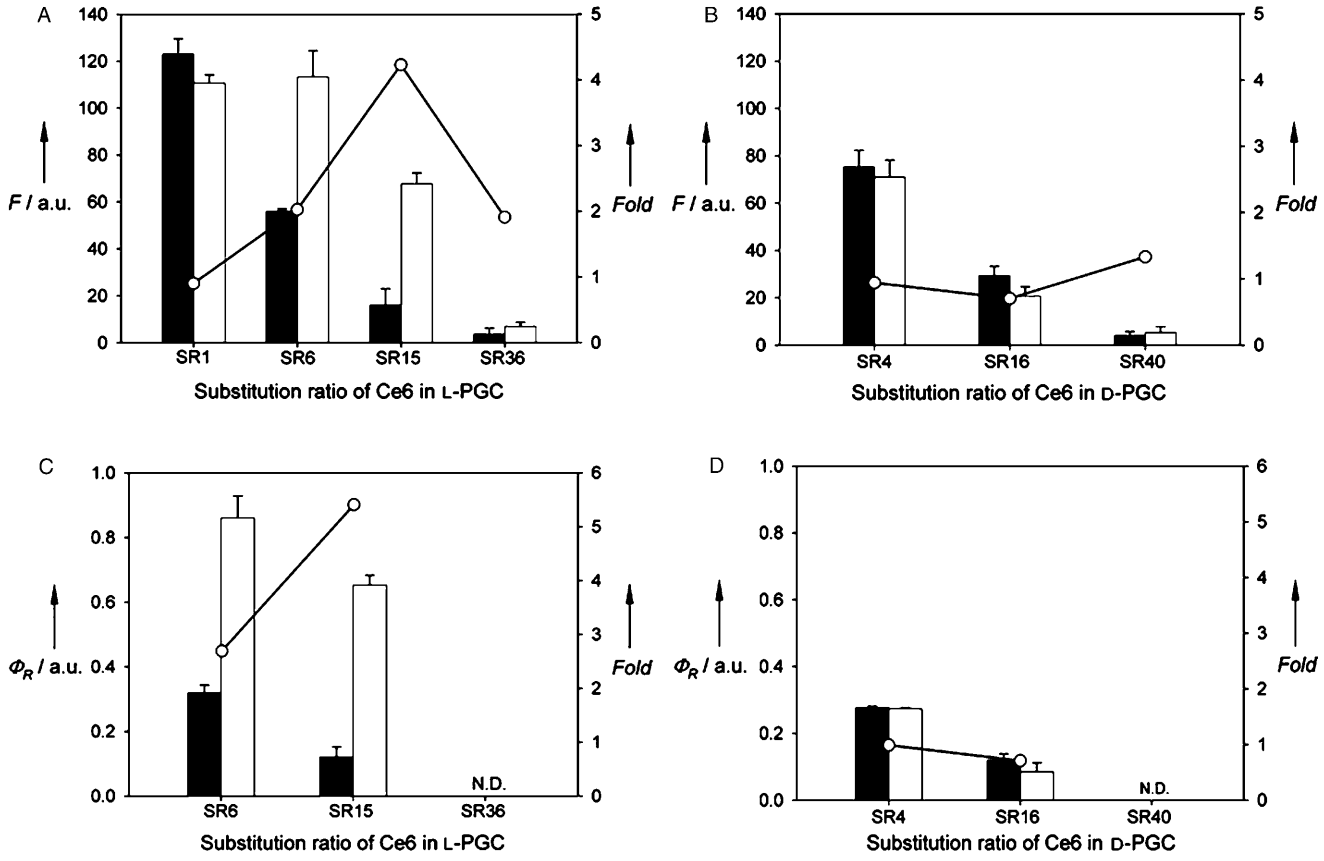

Figure 2. Trypsin-induced changes of fluorescence (A and B) and singlet oxygen generation (SOG; C and D). L-PGC conjugates (A and C) and D-PGC conjugates (B and D) treated with trypsin (open bars) or with phosphate buffer only (filled bars). Fluorescence was measured at $\lambda_{ex}=650$ nm and $\lambda_{em}=670$ nm, and the SOG was determined by irradiation at $\lambda=650$ nm. The *y*-axes show fold increase (○) in the fluorescence signal and SOG. Experiments were performed in triplicate, mean ± SD. N.D. = not determined.

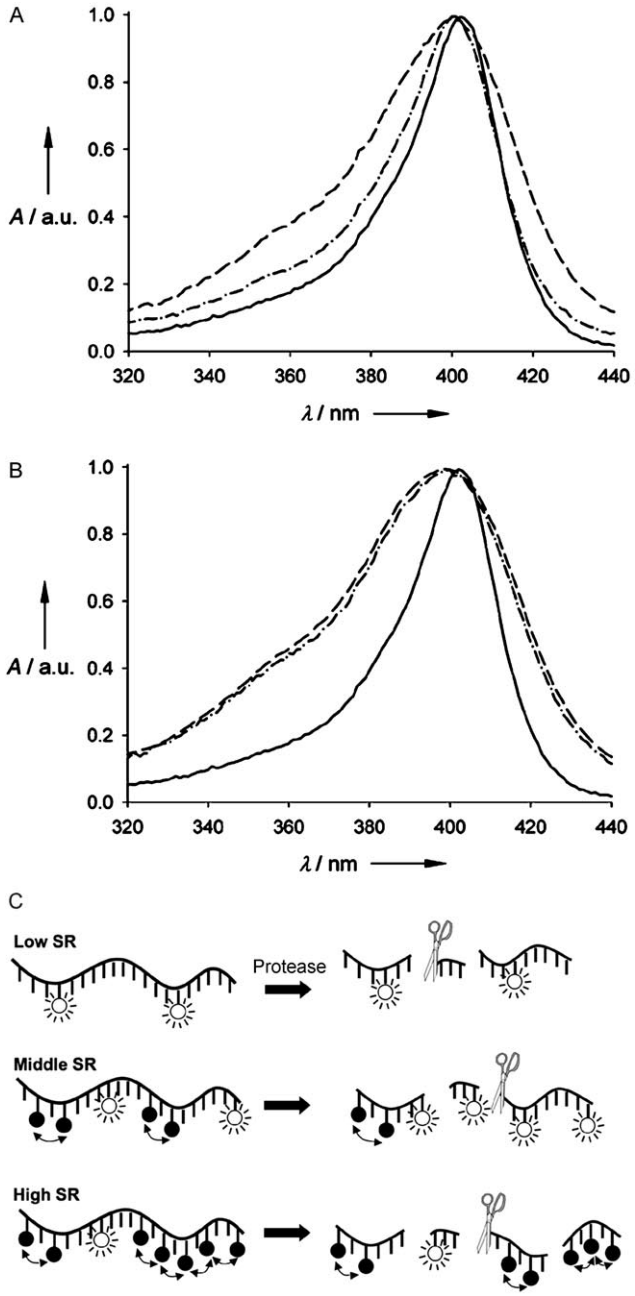

Figure 3. Normalized UV/Vis absorption spectra of A) L-SR15 and B) L-SR36. Spectra show conjugates (-----), trypsin-treated conjugates (–•–•), and free Ce6 (——) in phosphate buffer solution. C) SR-dependant fluorescence activation after enzyme treatment (arrow indicates energy transfer between photosensitizers).

creasing the SR of Ce6 in L-PGC, the number of free lysine residues in the poly-L-lysine backbone is decreased, resulting in fewer sites for enzymatic cleavage. This results in larger degradation products, which are still partially quenched (Figure 3c). This would explain why the fluorescence intensities and SOG were not fully recovered at higher SRs.

The activation of fluorescence signal was subsequently studied in cell culture. Previously, we demonstrated that the PGC backbone can be degraded by trypsin-like cysteine proteases, including cathepsins B, L, and S.[3] Incubation of HT1080 fibrosarcoma cells with the L-PGC conjugates at concentrations corresponding to 1 μM Ce6 for 4 h gave SR-dependant decreases in fluorescence intensity with increasing SR of L-PGC conjugates, as observed by confocal microscopy of the cells (Figure 4). No fluorescence signal was observed in the cells incubated with free Ce6. Previously, it was reported that the cellular uptake of porphyrin derivatives, including Ce6, is significantly lower in the presence of serum than it is in the absence of serum, because nonspecific binding to serum prevents intracellular uptake of the photosensitizers.[10,11] Therefore, the results reported herein indicate that conjugation of Ce6 with L-PGC is helpful to overcome this shortcoming. Prior studies indicate that up to 5% of the injected dose of PGC accumulates in tumors[12] as a result of the enhanced permeability and retention (EPR) effect.[13]

The correlation between fluorescence intensity and phototoxicity was further investigated in cell studies. From the in vitro phototoxicity study, L-PGC conjugates with lower SR showed better phototoxicity than those with higher SR. Cell viability (at a light dose of 10 J cm^{-2}) was 53.9 ± 3.1% for SR6, 70.5 ± 2.9% for SR15, 80.2 ± 1.1% for SR36, and 95.1 ± 6.4% for free Ce6 (Figure 5). Significant differences ($p < 0.01$) in cell viability were observed between all groups. The cell viability data correlated well with confocal microscopy data.

The above data indicate that chemical optimization is an essential step in preparing protease-mediated photosensitizers. Although the preparation with a high SR ratio, such as L-SR36, showed near complete quenching of fluorescence and SOG, it could also not be activated. L-SR15 showed the highest activation ratio of the conjugates tested in this study. This lead conjugate had only 12% phototoxicity in its initial state, but proteolysis increased its phototoxicity by greater than fivefold.

The results of this study show that the inhibition of SOG can be achieved by conjugating multiple Ce6 photosensitizers onto a polypeptide backbone, and that the photosensitivity of Ce6 can be recovered by proteolytic activity. We expect that higher increases in SOG after enzyme treatment and better enzyme selectivity can be obtained by inserting other protease-selective peptide substrates between the photosensitizers and the polymeric backbone, such as previously reported with protease-sensitive probes.[14] As porphyrin-based photosensitizers show fluorescence quenching and decreased SOG at increased concentration, this protease-mediated approach to PDT may be applied not only to Ce6 but also to other porphyrin derivatives. In addition, this protease-activated design may be useful to treat specific types of diseases in which a targeted protease is overexpressed, while prohibiting photosensitivity to normal tissues.

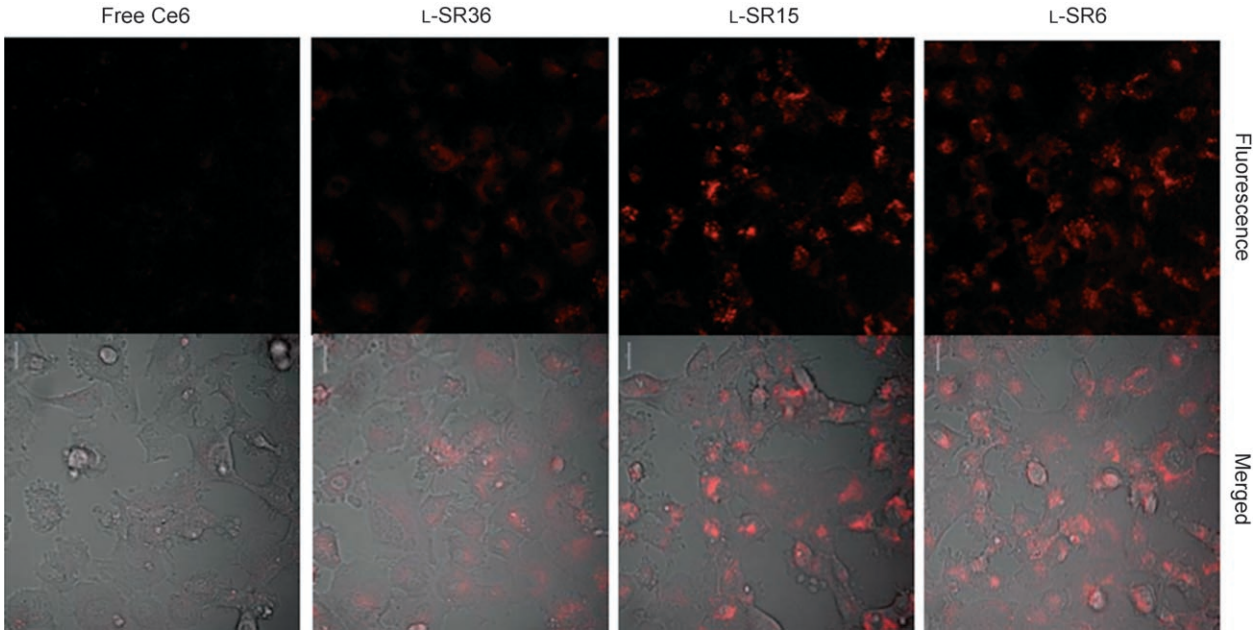

Figure 4. Confocal microscopy images of unfixed HT1080 cells incubated with free Ce6 or L-PGC conjugates (1 μM) with different SRs. Top row: fluorescence images of the cells. The fluorescence signals are from Ce6. Bottom row: transmitted light images merged with the fluorescence image above. Magnification: 40×.

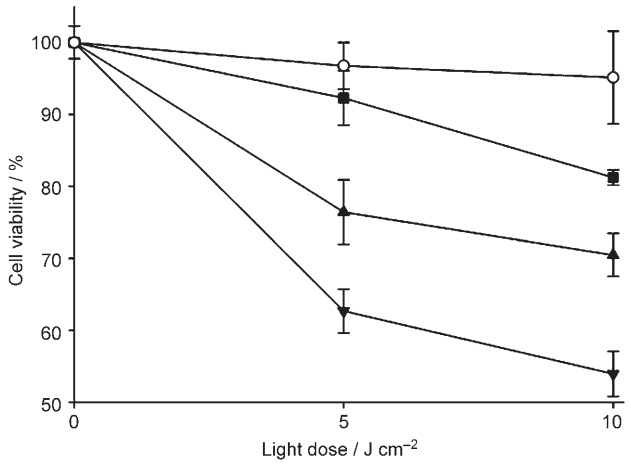

Figure 5. In vitro phototoxicity of free Ce6 and L-PGC conjugates. Photosensitizers (equivalent to 1 μM Ce6) were incubated for 4 h, then treated with laser light ($\lambda = 650$ nm, $n = 5$–6) at varying doses. Symbols represent cells incubated with free Ce6 (○), L-SR36 (■), L-SR15 (▲), and L-SR6 (▼). Significant differences ($p < 0.01$) in the cell viability were observed between all groups at both light doses (5 and 10 J cm^{-2}). Experiments were performed in triplicate, mean ± SD.

Acknowledgements

This research was supported in part by NIH P50-CA86355, RO1 CA99385, and DOD DC044945.

Keywords: fluorescence · photodynamic therapy · photosensitizers · proteases · quenching

[1] I. J. MacDonald, T. J. Dougherty, *J. Porphyrins Phthalocyanines* **2001**, *5*, 105.
[2] W. M. Sharman, J. E. van Lier, C. M. Allen, *Adv. Drug Delivery Rev.* **2004**, *56*, 53.
[3] R. Weissleder, C. H. Tung, U. Mahmood, A. Bogdanov, Jr., *Nat. Biotechnol.* **1999**, *17*, 375.
[4] J. R. Lakowicz, *Principles of fluorescence spectroscopy*, 2nd ed., Kluwer Academic, New York, **1999**.
[5] R. W. Redmond, E. J. Land, T. G. Truscott, *Adv. Exp. Med. Biol.* **1985**, *193*, 293.
[6] X. Damoiseau, H. J. Schuitmaker, J. W. Lagerberg, M. Hoebeke, *J. Photochem. Photobiol. B* **2001**, *60*, 50.
[7] M. R. Hamblin, J. L. Miller, I. Rizvi, B. Ortel, *J. X-Ray Sci. Technol.* **2002**, *10*, 139.
[8] B. M. Aveline, T. Hasan, R. W. Redmond, *J. Photochem. Photobiol. B* **1995**, *30*, 161.
[9] J. R. McCarthy, J. M. Perez, C. Bruckner, R. Weissleder, *Nano Lett.* **2005**, *5*, 2552.
[10] R. M. Bohmer, G. Morstyn, *Cancer Res.* **1985**, *45*, 5328.
[11] B. Cunderlikova, L. Gangeskar, J. Moan, *J. Photochem. Photobiol. B* **1999**, *53*, 81.
[12] E. Marecos, R. Weissleder, A. Bogdanov, Jr., *Bioconjugate Chem.* **1998**, *9*, 184.
[13] R. Satchi-Fainaro, M. Puder, J. W. Davies, H. T. Tran, D. A. Sampson, A. K. Greene, G. Corfas, J. Folkman, *Nat. Med.* **2004**, *10*, 255.
[14] C. H. Tung, S. Bredow, U. Mahmood, R. Weissleder, *Bioconjugate Chem.* **1999**, *10*, 892.

Received: February 7, 2006
Published online on May 10, 2006

CHEMMEDCHEM

DOI: 10.1002/cmdc.200500036

Conjugation of a Photosensitizer to an Oligoarginine-Based Cell-Penetrating Peptide Increases the Efficacy of Photodynamic Therapy

Yongdoo Choi, Jason R. McCarthy, Ralph Weissleder, and Ching-Hsuan Tung*[a]

To improve the efficiency of intracellular delivery of photosensitizers and the efficacy of photodynamic therapy, a membrane-penetrating arginine oligopeptide (R_7) was conjugated to 5-[4-carboxyphenyl]-10,15,20-triphenyl-2,3-dihydroxychlorin (TPC). The resulting conjugate (R_7–TPC) enhanced intracellular TPC uptake, which increased proportionally with the incubation time of the conjugate. The water solubility of the highly hydrophobic TPC photosensitizer was also improved after conjugation. Increased phototoxicity of R_7–TPC was observed after an incubation time of only 30 min. Tumor cells mainly underwent apoptosis at lower concentrations of the photosensitizer–polyarginine conjugate, whereas necrotic cell damage became prevalent at higher concentrations.

Introduction

Photodynamic therapy (PDT) is a relatively new modality for the treatment of cancers and other nonmalignant conditions.[1] It involves the administration of a photosensitizing agent, usually a porphyrin-based compound, and subsequent illumination of the tissue by a visible, nonthermal light source of the appropriate wavelength. This light exposure excites the photosensitizer, which is then able to interact with its surroundings. In oxygenated environments, the energy of the excited state is often dissipated by transfer to molecular oxygen, which leads to the formation of the highly reactive and cytotoxic singlet oxygen species. When this process occurs within tissues, it results in cellular damage.[2] As this effect is observed only in the presence of light, PDT is locally selective, thereby minimizing the damage to surrounding healthy tissue. When injected, porphyrin-based photosensitizers are found to be taken up by malignant or dysplastic tissues with some selectivity; however, the hydrophobic nature of photosensitizers often causes them to accumulate in healthy tissues, resulting in prolonged photosensitivity.[3] Cases of skin and eye photosensitivity have been observed in clinical trials, requiring patients to avoid sunlight exposure for several weeks or months.[1,3]

Cellular localization is important to the efficacy of PDT agents, as singlet oxygen has a short lifetime (<0.04 μs) and a radius of action (<0.02 μm) that is small in comparison with the diameter of tumor cells (≥ 10 μm).[4] Although many photosensitizers in current use tend to accumulate within the plasma membrane of cancer cells as a result of their lipophilicity,[5,6] some subcellular sites have been shown to be more sensitive to photodynamic damage than the plasma membrane.[7] Nevertheless, various delivery systems, such as nuclear localization signals and receptor targeting, have been suggested to enhance subcellular accumulation.[7,8]

Recently, arginine-rich peptides, originating from the HIV-1 Tat protein and other proteins, have been reported as cell-penetrating signals.[9] These oligoarginine peptides have been applied to the delivery of various chemical agents and drugs into cells.[9–11] Previous studies have demonstrated that the conjugation of *meso*-tetraphenylporphyrin to positively charged peptides containing up to three arginine residues showed increased cellular uptake, yet the photodynamic efficacy of this delivery system has not been demonstrated.[10] As it has been shown that longer polyarginine chains (heptamers and nonamers) undergo more efficient cellular uptake than do monomers, dimers, or trimers,[11,12] we hypothesized that the conjugation of an arginine heptamer oligopeptide (R_7) to a potent chlorin-based photosensitizer, 2,3-*vic*-dihydroxy-*meso*-tetraphenylchlorin,[13] would drastically increase the effectiveness of tumor cell killing by improving the aqueous solubility and cellular uptake of the conjugate. Thus, this novel class of cell-penetrating peptide-based photodynamic therapy agents may permit a decrease in the dose of photosensitizer required for the treatment of cancers.

Results

Synthesis and characterization of the photosensitizer–peptide conjugate

The photosensitizer used in this study was chosen for its optical properties and its reactivity. 5-[4-Carboxyphenyl]-10,15,20-

[a] *Dr. Y. Choi,[+] Dr. J. R. McCarthy,[+] Prof. Dr. R. Weissleder, Prof. Dr. C.-H. Tung*
Center for Molecular Imaging Research
Massachusetts General Hospital
Harvard Medical School
149 13th St., Rm. 5406, Charlestown, MA 02129 (USA)
Fax: (+1) 617-726-5708
E-mail: tung@helix.mgh.harvard.edu
[+] *These authors contributed equally to this work.*

triphenyl-2,3-dihydroxychlorin (TPC) was synthesized by the osmium tetroxide oxidation of the corresponding porphyrin (Scheme 1).[14] This reaction is one of the few known pathways by which a porphyrin can be directly converted into a chlorin,

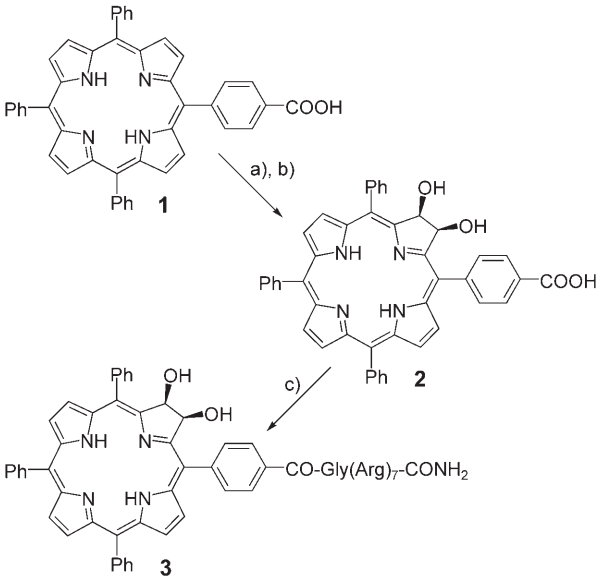

Scheme 1. Preparation of the R_7–TPC conjugate: a) OsO_4, pyridine; b) H_2S; c) solid-phase peptide synthesis.

and as such, is more efficient than other multi-step, total syntheses of chlorins or extraction from natural sources.[15] TPC was purified by HPLC, as column chromatography with silica gel was rendered unsuccessful from impurities of similar polarity. The identity of the product was confirmed by mass spectrometry ($m/z = 693.2492$ $[M+H]^+$) and ^1H and ^{13}C NMR spectroscopy. The ^1H NMR spectra showed peaks characteristic of diol chlorins, namely a singlet at 3.3 ppm, which is exchangeable with D_2O and attributable to the protons of the hydroxy groups, and a singlet at 6.5 ppm that corresponds to the methynic protons of the partially saturated pyrrolic ring. In the ^{13}C NMR spectra, the carbon atoms of the partially saturated pyrrolic ring are observed at 74 ppm, while the resonance for the carbon atom of the acid moiety is at 168 ppm. Purified TPC was coupled to the N terminus of the arginine oligopeptide on solid support. The final R_7–TPC product was purified by HPLC and confirmed by MALDI-TOF mass spectrometry ($m/z =$ 1842 $[M+H]^+$).

The UV/Vis spectrum of TPC (Figure 1 A) is similar to that observed for analogous chlorins, having a broadened Soret band with a slightly lower extinction coefficient (1.0×10^5 L mol^{-1} cm^{-1}) than that of the starting porphyrin (1.6×10^5 L mol^{-1} cm^{-1}). Moreover, the longest-wavelength side band for TPC is sevenfold greater than that of porphyrin (1.5×10^4 L mol^{-1} cm^{-1} for TPC versus 2.0×10^3 L mol^{-1} cm^{-1} for the starting porphyrin). Surprisingly, upon TPC conjugation to the oligopeptide, the extinction coefficient of the Soret band increases (1.6×10^5 L mol^{-1} cm^{-1}, Figure 1 B). This contrasts with what is usually observed for the dissolution of relatively hydrophobic porphyrins in aqueous solution, as aggregation often occurs and leads to decreased and broadened absorption.[16] This may indicate that the conjugation of TPC to the peptide results in a product that is favorably solvated, although there is a slight decrease ($\approx$33 %) in the extinction coefficient of the longest-wavelength side band (1.0×10^4 L mol^{-1} cm^{-1}).

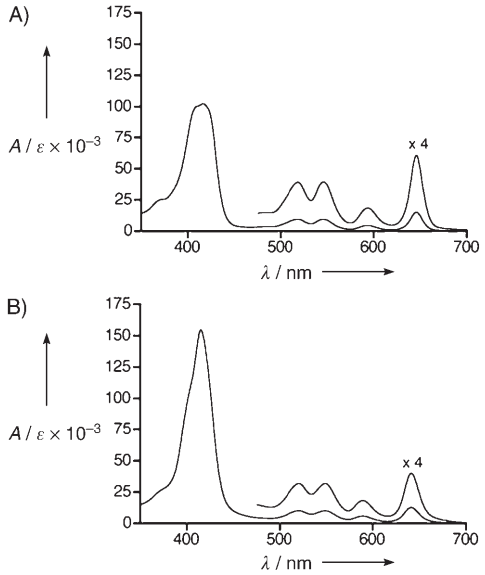

Figure 1. UV/Vis spectra of A) TPC in CH_2Cl_2/MeOH (99:1 *v/v*), and B) R_7–TPC in water.

Singlet oxygen quantum yields (ϕ_Δ) were calculated for both TPC and R_7–TPC with 1,3-diphenylisobenzofuran (DPBF) as the probe molecule in *N*,*N*-dimethylformamide (DMF) (Table 1).[17,18] DPBF, a fluorophore, has been shown to chemically quench singlet oxygen to yield a nonfluorescent species. Therefore, the singlet oxygen quantum yield for each compound was obtained by comparing the initial slope of the decrease in fluorescence intensity versus time for the molecule of interest against that of a standard. The singlet oxygen quantum yield was not altered after conjugation, which indicates that phototoxicity was retained.

Table 1. Physical properties of chlorins used in this study and the corresponding singlet oxygen quantum yields.

Compd	λ_{max} [nm]	log ε[a]	ϕ_Δ
TPC	646[b]	4.18	0.65[e]
R_7–TPC	642[c]	4.00	0.69[e]
chlorin e6	664[d]	4.60	0.75[f]

[a] Extinction coefficients are for the longest-wavelength absorptions. [b] In CH_2Cl_2/MeOH (99:1 *v/v*). [c] In H_2O. [d] In acetone. [e] In DMF. [f] In phosphate-buffered saline.[27,28]

Cellular uptake of photosensitizers

Cellular uptake of the photosensitizers chlorin e6 (C_{e6}) and R_7–TPC was quantified by fluorescence measurement at different

time points (Figure 2). It was found that only a trace amount of C_{e6} was taken up by MDA-MB-468 cells, and that longer incubation times did not lead to improved internalization. However, R_7–TPC showed an almost linear relationship between

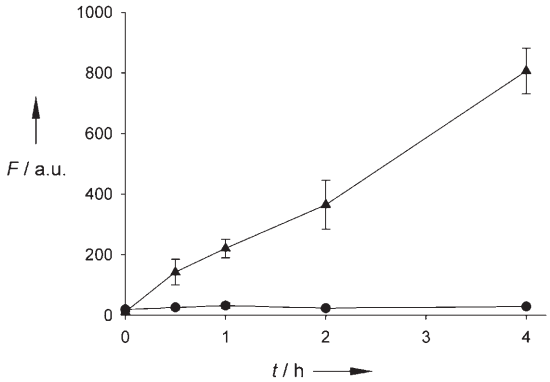

Figure 2. Intracellular uptake of C_{e6} (●) and R_7–TPC (▲) at different incubation times. Photosensitizers were dissolved in serum containing growth medium at a final concentration of 1 μM and distributed to a 24-well plate for 30 min, 1 h, 2 h, and 4 h ($n=4$, a.u.: arbitrary units).

uptake and incubation time. About 5.78 ± 0.55 % of the added conjugate was internalized within 4 hours as determined by calculation from a calibrated standard solution. In contrast, the cells took up only 0.06 ± 0.03 % of C_{e6} within 4 hours. Internal distribution of R_7–TPC was further observed by confocal microscopy (Figure 3). In less than 30 min, a characteristic endosomal distribution of the conjugate was observed. Longer incubation led to greater accumulation in the cell. In particular, a significant amount of R_7–TPC was found along the nuclear membrane, but not within the nucleus. As expected, minimal fluorescence was observed for cells incubated with C_{e6}. However, during image acquisition, changes in cell morphology were observed (Figure 3). Repetitive laser scanning of cells may excite the photosensitizers and thus cause cell damage.

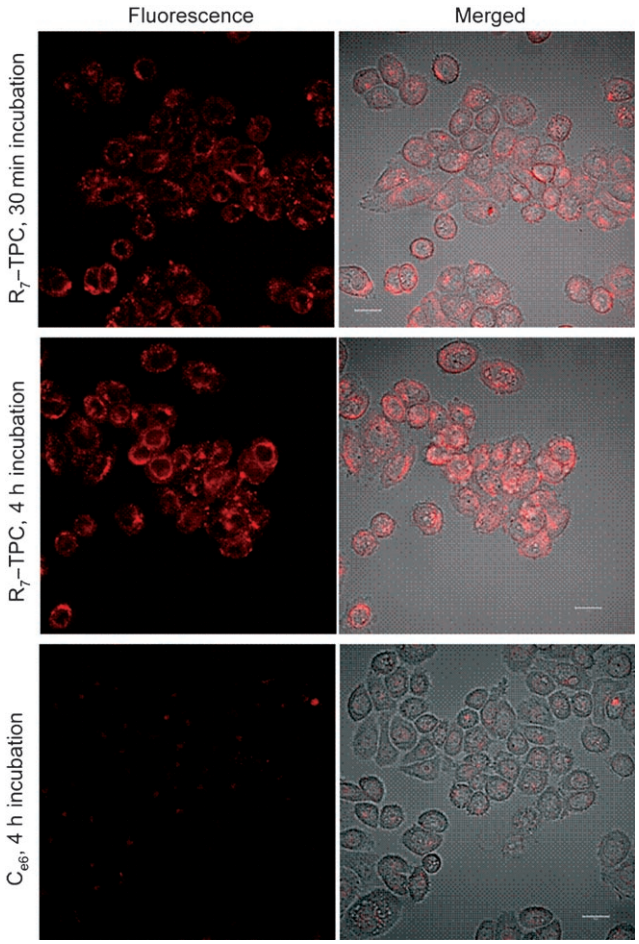

Figure 3. Confocal microscopy images of unfixed MDA-MB-468 cells incubated with C_{e6} or R_7–TPC (1 μM) at various incubation times. Left column: fluorescence images; fluorescence signals were from chlorin. Right column: Transmitted light images merged with the respective fluorescence image. Magnification: 40×; scale bars: 20 μm.

Light-induced phototoxicity

To demonstrate the effectiveness of PDT with the R_7–TPC conjugate, cells were incubated with C_{e6} or R_7–TPC (1 μM) for various times. After incubation, the cells were washed, illuminated with light, and then incubated for an additional 24 hours. Cell survival was then determined with an MTT assay. For the R_7–TPC treated groups, cell survival rates were 20.5 ± 3.7, 13.7 ± 2.7, 10.1 ± 1.7, and 11.5 ± 3.4 % for 0.5, 1, 2, and 4 hours incubation time, respectively (Figure 4). As expected, cells incubated with C_{e6} showed no significant cell death. At the tested concentrations of both photosensitizers, dark toxicity was not observed in the absence of light exposure (data not shown). Cells incubated with the R_7 peptide for 4 hours and treated with light also showed no cell death, which indicates that R_7 alone does not affect cell viability.

The possible pathways of cell damage were studied by staining the cells with Hoechst 33342 and PI fluorescent dyes. The Hoechst dye is known to stain all nuclei, whereas PI only stains

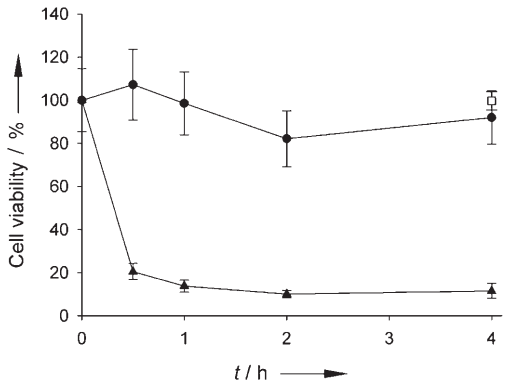

Figure 4. Phototoxicity at varying incubation times for R_7 (□), R_7–TPC (▲), and C_{e6} (●). Cells were incubated with photosensitizers (1 μM) for 0.5, 1, 2, and 4 h, then treated with laser light ($\lambda=650$ nm, $n=4$). Cells were treated with R_7 (1 μM) for 4 h, then exposed to light ($n=4$). Cell survival rate was measured by the MTT assay. Significant difference ($p<0.01$) in cell viability between groups treated with C_{e6} and R_7–TPC was observed at all incubation time points.

necrotic cells. As shown in Figure 5, cells treated with R_7–TPC plus PDT show intense nuclear PI signal, which indicates necrosis. As expected, longer incubation with R_7–TPC induced more cell necrosis (Figure 6). Incubation times of 0.5, 1, 2, and 4 hours gave 7.9, 17.8, 40.9, and 98.4% necrotic cells, respectively. In contrast, PI signal was not observed in the cells incubated with C_{e6} (Figure 5 and 6B). Only 1.2% of the cells were damaged under treatment with C_{e6} for 4 hours and exposure to light. Less than 0.1% of the necrotic damage was observed for cells treated with either light or photosensitizers alone.

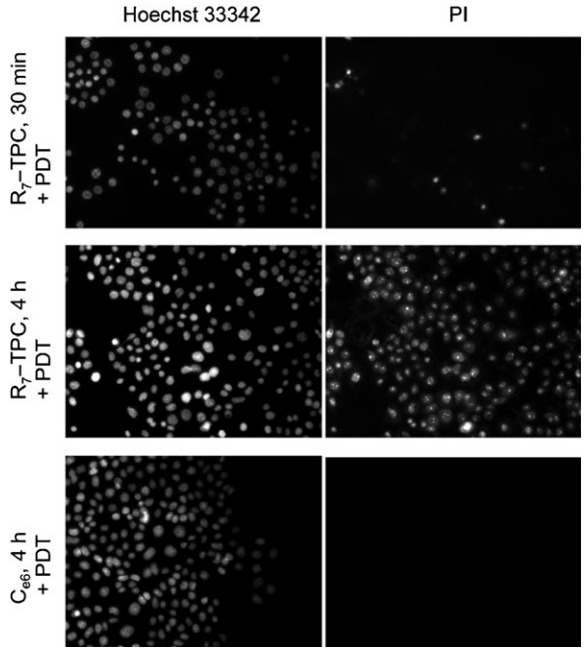

Figure 5. Representative fluorescence microscopy images illustrating necrotic cell damage, which occurred during PDT. Cells were stained with both Hoechst 33342 (left column) and PI (right column) immediately after PDT.

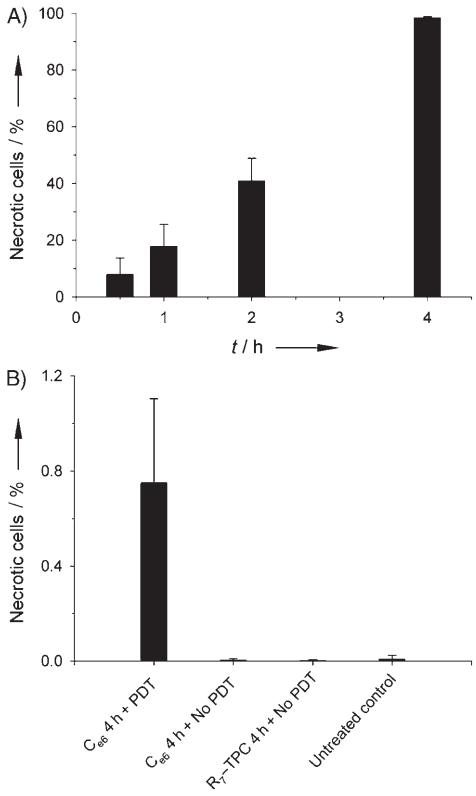

Figure 6. Quantitation of necrotic cells ($n = 3$). A) Necrotic damage to the cells treated with R_7–TPC (1 μM) for varying incubation times; cells were stained with Hoechst 33342 and PI immediately after PDT to quantify necrotic damage of the cells. B) Necrotic damage for C_{e6}-treated and control groups. Dark toxicity of cells incubated with photosensitizers or cell growth media for 4 h without light treatment showed no sign of necrosis.

Discussion

The hydrophobic nature of most photosensitizers limits their application in vivo. Special formulations, such as mixtures of ethanol/polyethylene glycol 400/water, have been proposed for the administration of hydrophobic photosensitizers.[19] TPC, for example, is completely water-insoluble and as such, has little clinical relevance. Our approach of appending an R_7 oligopeptide to TPC improves not only the delivery, but also the aqueous solubility of the sensitizer. The solubility of the R_7–TPC conjugate in phosphate buffered saline (pH 7.4) is greater than 10 mM.

The uptake of R_7–TPC was observed to have a near-linear relationship with concentration in the presence of 10% FBS, whereas the uptake of C_{e6} was negligible even after 4 hours of incubation (Figure 2). It has been reported previously that the cellular uptake of photosensitizers, including C_{e6}, is significantly lower in the presence of serum than it is in the absence of serum as a result of nonspecific binding to serum components.[20–22] Our results indicate that the R_7 oligopeptide conjugated TPC overcomes this limitation and allows effective cellular uptake.

Confocal microscopy shows that the R_7–TPC conjugate enters cells efficiently, as the fluorescence of R_7–TPC was observed in almost all cells after an incubation time of only 30 min (Figure 3). Photodynamic treatment of these cells with light ($\lambda = 650$ nm) caused necrotic membrane damage of 8% of the cells, as observed by staining with Hoechst 33342 and PI immediately after light exposure (Figures 5 and 6). However, MTT assay results showed that about 80% of the cells were nonviable 24 hours later (Figure 4). We therefore conclude that approximately 70% of cell death occurred through an apoptotic mechanism, as PDT is known to elicit both necrosis and apoptosis, depending on the sensitizer used and its subcellular localization. By increasing incubation time to 4 hours, the cellular concentration of R_7–TPC was increased by about sixfold; most cells then turned necrotic upon treatment with light. As photodamage is limited to within 0.02 μm of the site of photoactivation owing to the short half-life of reactive singlet oxygen (< 0.04 μsec),[4] our results indicate that low concentrations of R_7–TPC induce apoptosis, yet higher concentrations of R_7–TPC are needed to cause necrosis.

In summary, the therapeutic efficiency of a photosensitizer can be significantly improved by conjugation to a cell-pene-

trating peptide, as has been demonstrated. The highly charged R_7 oligopeptide not only imparts solubility to the hydrophobic TPC in aqueous solution, but also transports TPC into cells. Following illumination with light of the appropriate wavelength, the internalized conjugate is able to kill cells through both necrotic and apoptotic pathways, depending on the concentration of the sensitizer.

Experimental Section

General. All solvents and reagents were reagent grade and used as received. HPLC was performed with a Vydac 218TP Series C-18 reversed-phase column (particle size = 10 μm, i.d. = 22 mm, *l* = 250 mm). Buffer A consisted of 0.1% trifluoroacetic acid (TFA) in deionized water; buffer B was acetonitrile/buffer A (9:1 *v/v*). UV/Vis spectra were recorded on a Cary 50 spectrophotometer (Varian, Palo Alto, CA) and fluorescence spectra, on a Hitachi F-4500 fluorescence spectrophotometer (Danbury, CT, USA).

5-[4-Carboxyphenyl]-10,15,20-triphenyl-2,3-dihydroxychlorin (compound 2). The synthesis of TPC **2** was performed as described by Brückner et al.[14] (Scheme 1). OsO_4 (250 mg, 0.984 mmol) was added to a solution of 5-(4-carboxyphenyl)-10,15,20-triphenylporphyrin **1**[23] (500 mg, 0.760 mmol) in CH_2Cl_2/pyridine (3:1 *v/v*, 100 mL). The flask was sealed, and the reaction proceeded for 48 h. H_2S gas was then bubbled through the solution for 5 min. The system was closed again for 45 min, after which time N_2 was bubbled through the system to purge off extraneous H_2S. The solution was evaporated to dryness in vacuo, dissolved in buffer B, and purified by preparative HPLC by using a linear gradient from 65% buffer B to 80% buffer B over 45 min at a flow rate of 6 mL min^{-1}. The product eluted at $t_R = 18$ min. The fractions containing the product were combined and evaporated to dryness to yield TPC as a green-purple film. Purity was assessed by analytical HPLC, and a Beer's law plot was used to determine the extinction coefficients of the product. R_f (silica, CH_2Cl_2/MeOH (95:5 *v/v*)): 0.20; UV/Vis (CH_2Cl_2/MeOH (99:1 *v/v*)) λ_{max} (log ε): 416 (5.01), 517 (3.98), 546 (3.98), 594 (3.67), 646 nm (4.18) (Figure 1); ^{1}H NMR (400 MHz, [D$_7$]DMF): $\delta = -1.74$ (s, 2H), 6.36 (s, 2H), 7.73–7.77 (m, 6H), 7.83–7.86 (m, 4H), 8.21–8.24 (m, 4H), 8.33–8.40 (m, 2H), 8.43–8.48 (m, 4H), 8.51 (s, 2H), 8.75 (d, $J = 4.9$ Hz, 1H), 8.79 ppm (d, $J = 5.0$ Hz, 1H); ^{13}C NMR (100 MHz, [D$_7$]DMF): $\delta = 74.0$, 74.1, 114.5, 114.6, 121.1, 122.5, 124.7, 124.9, 127.1, 127.4, 127.9, 128.1, 130.8, 132.1, 132.3, 132.6, 134.0, 134.3, 134.9, 135.4, 140.6, 141.7, 146.2, 152.1, 152.7, 164.5, 164.6, 167.6 ppm; ESI MS (70 V, CH_3CN) *m/z* $[M+H]^+$: 693; HRMS (ES+ of $[M+H]^+$) calcd for $C_{45}H_{32}N_4O_4$: 693.2496, found: 693.2492.

Arginine oligopeptide synthesis and R_7–TPC conjugation (compound 3). Synthesis of peptide GR_7 was performed on an automated solid-phase peptide synthesizer (433A, Applied Biosystems, Foster City, CA, USA) by using the traditional Fmoc (9-fluorenylmethyloxycarbonyl) methodology on Rink amide resin (405 mg, 0.25 mmol). All amino acids, Fmoc–Gly and Fmoc–Arg(Pbf) (4 equiv; Pbf = 2,2,4,6,7-pentamethyldihydrobenzofuran-5-sulfonyl) were attached to the Rink amide (0.1 mmol) resin by stepwise elongation using 2(1*H*-benzotriazole-1-yl)-1,1,3,3-tetramethyluronium hexafluorophosphate (HBTU, 4 equiv)/*N*-hydroxybenzotriazole (HOBt, 4 equiv)/*N*-methyl morpholine (8 equiv) as the coupling reagents in DMF (10 mL). Upon completion of synthesis, TPC (30 mg, 0.043 mmol, 0.87 equiv) was added to the resin-bound peptide (0.05 mmol) in DMF (4 mL). The resin was allowed to swell for 15 min, at which time HOBt (6.8 mg, 0.05 mmol, 1 equiv), HBTU (18 mg, 0.05 mmol, 1 equiv), and diisopropylethylamine (DIPEA, 1 mL) were added. The reaction proceeded for 16 h, at which point it was filtered to collect the resin-peptide conjugate. This was then washed twice with CH_2Cl_2 and twice with methanol to remove excess reagents. The conjugate was cleaved from the resin with TFA/triisopropylsilane (TIS)/H_2O (95:2.5:2.5 *v/v/v*), filtered to remove the resin, and precipitated in methyl *tert*-butyl ether. The precipitate was dissolved in buffer A and purified by HPLC using a linear gradient of buffer B (20→80%, 45 min, flow rate = 6 mL min^{-1}). The product eluted at 22 min, and fractions containing the product were combined and lyophilized to yield R_7–TPC as a green powder (23 mg, 0.012 mmol, 29%): UV/Vis (H_2O) λ_{max} (log ε): 416 (5.19), 520 (3.90), 549 (3.90), 589 (3.65), 642 nm (4.00) (Figure 1); MALDI-TOF MS *m/z* $[M+H]^+$: 1842.

Singlet oxygen quantum yields. Quantum yields were calculated by using a modification of the technique described by Kochevar and Redmond.[17] In brief, stock solutions of the photosensitizers with optical densities of 0.03, as well as a solution of 1,3-diphenylisobenzofuran (DPBF, 0.25 M), all in DMF, were mixed and kept in the dark. Stock solution of the photosensitizer (2.0 mL) containing the DPBF solution (8 μL, final concentration, 1 mM) was added into a fluorescence cuvette before irradiation at $\lambda = 650$ nm (60 mW) in a fluorescence spectrophotometer under constant stirring. Simultaneously, the fluorescence emission intensity of DPBF was monitored (excitation $\lambda = 471$ nm, emission $\lambda = 495$ nm). Singlet oxygen quantum yields were then calculated from the initial slope of the decrease in fluorescence intensity with the following equation:

$$\Phi_\Delta(U) = \Phi_\Delta(St) \times {}^{S(U)}/_{S(St)}$$

in which *U* and *St* denote unknown and standard, and *S* represents the slope. *meso*-Tetraphenylporphyrin was used as the standard.

Cellular uptake. MDA-MB-468 cells (human breast carcinoma, American Type Culture Collection, Manassas, VA, USA) were maintained in Dulbecco's medium (DMEM, Cellgro, Mediatech, Washington DC, USA) supplemented with 10% fetal bovine serum (FBS, Cellgro) and 1% penicillin/streptomycin at 37 °C under a humidified atmosphere with 5% CO_2. Cellular uptake of photosensitizers was measured as previously published, with slight modification.[24] MDA-MB-468 cells (10^5 cells) in DMEM (1 mL) with FBS (10%) were seeded into each well of 24-well plates and incubated at 37 °C in a humidified CO_2 atmosphere (5%) for 24 h. Fresh medium with FBS (10%) containing either C_{e6} or R_7–TPC (1 μM, 1 mL) was added, and cells were incubated for 30 min, 1 h, 2 h, or 4 h. The cells were then washed three times with Hank's balanced salt solution (HBSS, Mediatech, Herndon, VA, USA) and dissociated from the plates by incubating the cells with trypsin–EDTA (1 mL) for 15 min at 37 °C. The resulting cell suspension was centrifuged, and the cell pellets were then dissolved in a solution of sodium hydroxide (0.1 M, 1.5 mL)/sodium dodecyl sulfate (SDS, 1%) for at least 24 h at room temperature to give a homogeneous solution. The fluorescence was measured and compared with a standard curve. Standard solutions of C_{e6} and R_7–TPC at known concentrations were prepared in 0.1 M NaOH/1% SDS, and the fluorescence of the solutions was measured after 24 h incubation at room temperature.

Cellular distribution by confocal microscopy. MDA-MB-468 cells (10^5 cells) in DMEM (0.5 mL) with FBS (10%) were seeded into each well of a Lab-Tek II chambered cover glass (Nalge Nunc, Naperville, IL, USA) and incubated at 37 °C in a humidified atmosphere (5% CO_2) for 24 h. C_{e6} or R_7–TPC were dissolved in fresh DMEM medium with 10% FBS (1 μM, 0.5 mL), added to the cells, and incubated for 30 min or 4 h. The cells were washed three times with HBSS before

imaging, and intracellular drug uptake was observed with a confocal microscope (Zeiss Axiovert 200, Thornwood, NY, USA) fitted with a Zeiss LSM Pascal Vario Laser Module (argon, 458/488/514 nm; HeNe, 543/633 nm). The HeNe laser ($\lambda = 543$ nm) paired with a long-pass emission filter for $\lambda = 650$ nm was used to visualize photosensitizers inside cells. It has been reported previously that fixation could affect cellular distribution.[25] Therefore, all experiments were performed with live cells without fixation.

Cell damage during PDT. MDA-MB-468 cells (10^5 cells) in DMEM (1 mL) with FBS (10%) were seeded into each well of 24-well plates and incubated at 37 °C in a humidified atmosphere (5% CO_2) for 24 h. Fresh medium with 10% FBS, containing C_{e6} or R_7–TPC (1 μM, 1 mL) was added, and the cells were incubated for 30 min, 1 h, 2 h, or 4 h. Thereafter, cells were washed three times with HBSS, fresh medium was added, and the cells were exposed to light ($\lambda = 650$ nm) delivered from a diode laser (B&W TEK, Newark, DE, USA) to give a total fluence of 10 J cm^{-2} at 42.1 mW cm^{-2}. To investigate the necrotic damage of cell membranes during PDT, nuclei of the cells were stained with Hoechst 33342 and propidium iodide (PI). The stained cells were then viewed in phase-contrast or fluorescence mode with an inverted epifluorescence microscope (Zeiss Axiovert, Thornwood, NY, USA). A cooled CCD camera (Sensys Photometrics, Tucson, AZ, USA) adapted with a narrow-bandpass filter was used for image capture. Three wells were used for each experimental group, with at least 350 cells in four random fields counted on each well. Cells without photosensitizer or cells with photosensitizer but without light illumination were also stained for comparison.

Cell survival assay at 24 h post-PDT. In total, 5000 cells in 0.2 mL DMEM with 10% FBS were seeded in each well of 96-well plates and cultured for 24 h until 70% confluent. The cells were incubated with fresh complete medium containing R_7, R_7–TPC or C_{e6} (1 μM, 0.2 mL) for different time periods. Thereafter, the cells were washed three times with HBSS, fresh medium was added, and the cells were exposed to light ($\lambda = 650$ nm) delivered from a diode laser to give a total fluence of 10 J cm^{-2} at 42.1 mW cm^{-2}. Cells were then incubated for a further 24 h, and the MTT microculture assay was used to measure cell viability (MTT = 3-[4,5-dimethylthiazol-2-yl]-2,5-diphenyltetrazolium bromide).[26] Untreated cells served as the gauge for 100% viability, whereas media served as background. Cells incubated with photosensitizers for 4 h but without light illumination were also evaluated.

Statistical analysis. The mean ± SD values were used for the expression of data. Statistical analyses of data were performed by using the Student *t* test. Differences were considered statistically significant with $p < 0.05$.

Acknowledgements

This research was supported by NIH grants P50-CA86355 and RO1-CA99385 and DOD grant BC044945. We thank Dr. Martha Morton for her assistance with NMR spectroscopic characterization.

Keywords: arginine · chlorin e6 · membranes · peptides · photodynamic therapy

[1] S. B. Brown, E. A. Brown, I. Walker, *Lancet Oncol.* **2004**, *5*, 497–508.
[2] I. J. MacDonald, T. J. Dougherty, *J. Porphyrins Phthalocyanines* **2001**, *5*, 105–129.
[3] R. Ackroyd, C. Kelty, N. Brown, M. Reed, *Photochem. Photobiol.* **2001**, *74*, 656–669.
[4] J. Moan, K. Berg, *Photochem. Photobiol.* **1991**, *53*, 549–553.
[5] M. Canete, A. Villanueva, V. Dominguez, S. Polo, A. Juarranz, J. C. Stockert, *Int. J. Oncol.* **1998**, *13*, 497–504.
[6] W. G. Roberts, M. W. Berns, *Lasers Surg. Med.* **1989**, *9*, 90–101.
[7] W. M. Sharman, J. E. van Lier, C. M. Allen, *Adv. Drug Delivery Rev.* **2004**, *56*, 53–76.
[8] T. V. Akhlynina, D. A. Jans, A. A. Rosenkranz, N. V. Statsyuk, I. Y. Balashova, G. Toth, I. Pavo, A. B. Rubin, A. S. Sobolev, *J. Biol. Chem.* **1997**, *272*, 20328–20331.
[9] C. H. Tung, R. Weissleder, *Adv. Drug Delivery Rev.* **2003**, *55*, 281–294.
[10] M. Sibrian-Vazquez, T. J. Jensen, F. R. Fronczek, R. P. Hammer, M. G. Vicente, *Bioconjugate Chem.* **2005**, *16*, 852–863.
[11] P. A. Wender, D. J. Mitchell, K. Pattabiraman, E. T. Pelkey, L. Steinman, J. B. Rothbard, *Proc. Natl. Acad. Sci. USA* **2000**, *97*, 13003–13008.
[12] D. J. Mitchell, D. T. Kim, L. Steinman, C. G. Fathman, J. B. Rothbard, *J. Pept. Res.* **2000**, *56*, 318–325.
[13] J. K. MacAlpine, R. Boch, D. Dolphin, *J. Porphyrins Phthalocyanines* **2002**, *6*, 146–155.
[14] C. Brückner, D. Dolphin, *Tetrahedron Lett.* **1995**, *36*, 3295–3298.
[15] R. B. Woodward, W. A. Ayer, J. M. Beaton, F. Bickelhaupt, R. Bonnett, P. Buchschacher, G. L. Closs, H. Dutler, J. Hannah, F. P. Hauck, S. Ito, A. Langemann, E. Le Goff, W. Leimgruber, W. Lwowski, J. Sauer, Z. Valenta, H. Volz, *Tetrahedron* **1990**, *46*, 7599–7659.
[16] S. Rahimipour, N. Ben-Aroya, K. Ziv, A. Chen, M. Fridkin, Y. Koch, *J. Med. Chem.* **2003**, *46*, 3965–3974.
[17] I. E. Kochevar, R. W. Redmond, *Methods Enzymol.* **2000**, *319*, 20–28.
[18] S. A. Gerhardt, J. W. Lewis, J. Z. Zhang, R. Bonnett, K. A. McManus, *Photochem. Photobiol. Sci.* **2003**, *2*, 934–938.
[19] L. Bourre, G. Simonneaux, Y. Ferrand, S. Thibaut, Y. Lajat, T. Patrice, *J. Photochem. Photobiol. B* **2003**, *69*, 179–192.
[20] R. M. Bohmer, G. Morstyn, *Cancer Res.* **1985**, *45*, 5328–5334.
[21] B. Cunderlikova, L. Gangeskar, J. Moan, *J. Photochem. Photobiol. B* **1999**, *53*, 81–90.
[22] M. O. Obochi, R. W. Boyle, J. E. van Lier, *Photochem. Photobiol.* **1993**, *57*, 634–640.
[23] D. A. James, N. Swamy, N. Paz, R. N. Hanson, R. Ray, *Bioorg. Med. Chem. Lett.* **1999**, *9*, 2379–2384.
[24] M. R. Hamblin, J. L. Miller, I. Rizvi, B. Ortel, E. V. Maytin, T. Hasan, *Cancer Res.* **2001**, *61*, 7155–7162.
[25] J. P. Richard, K. Melikov, E. Vives, C. Ramos, B. Verbeure, M. J. Gait, L. V. Chernomordik, B. Lebleu, *J. Biol. Chem.* **2003**, *278*, 585–590.
[26] J. L. Merlin, S. Azzi, D. Lignon, C. Ramacci, N. Zeghari, F. Guillemin, *Eur. J. Cancer Part A* **1992**, *28*, 1452–1458.
[27] T. Ando, K. Irie, K. Koshimizu, T. Takemura, H. Nishino, A. Iwashima, S. Nakajima, I. Sakata, *Tetrahedron* **1990**, *46*, 5921–5930.
[28] J. M. Fernandez, M. D. Bilgin, L. I. Grossweiner, *J. Photochem. Photobiol. B* **1997**, *37*, 131–140.

Received: September 2, 2005
Revised: November 18, 2005
Published online on January 24, 2006

